Geochemistry Geophysics Geosystems G3
AN ELECTRONIC JOURNAL OF THE EARTH SCIENCES
Published by AGU and the Geochemical Society

*Article*
Volume 9, Number 1
12 January 2008
Q01P23, doi:10.1029/2006GC001564
ISSN: 1525-2027

# Foraminiferal Mg/Ca increase in the Caribbean during the Pliocene: Western Atlantic Warm Pool formation, salinity influence, or diagenetic overprint?

**Jeroen Groeneveld**
*IFM-Geomar, Leibniz Institute of Marine Sciences, D-24148 Kiel, Germany*

*Now at Research Center of Ocean Margins, Bremen University, Leobener Strasse, D-28213 Bremen, Germany (jgroeneveld@uni-bremen.de)*

**Dirk Nürnberg**
*IFM-Geomar, Leibniz Institute of Marine Sciences, D-24148 Kiel, Germany*

**Ralf Tiedemann**
*IFM-Geomar, Leibniz Institute of Marine Sciences, D-24148 Kiel, Germany*

*Now at AWI, Institute for Polar and Marine Research, D-27515 Bremerhaven, Germany*

**Gert-Jan Reichart**
*Now at AWI, Institute for Polar and Marine Research, D-27515 Bremerhaven, Germany*

*Faculty of Earth Sciences, Utrecht University, 3508 TA Utrecht, Netherlands*

**Silke Steph**
*IFM-Geomar, Leibniz Institute of Marine Sciences, D-24148 Kiel, Germany*

*Now at AWI, Institute for Polar and Marine Research, D-27515 Bremerhaven, Germany*

**Lars Reuning**
*IFM-Geomar, Leibniz Institute of Marine Sciences, D-24148 Kiel, Germany*

*Now at RWTH Aachen, D-52062 Aachen, Germany*

**Daniela Crudeli**
*Institute of Geosciences, University of Kiel, D-24148 Kiel, Germany*

**Paul Mason**
*Faculty of Earth Sciences, Utrecht University, 3508 TA Utrecht, Netherlands*

[1] We constructed a high-resolution Mg/Ca record on the planktonic foraminifer *Globigerinoides sacculifer* in order to explore the change in sea surface temperature (SST) due to the shoaling of the Isthmus of Panama as well as the impact of secondary factors like diagenesis and large salinity fluctuations. The study covers the latest Miocene and the early Pliocene (5.6–3.9 Ma) and was combined with $\delta^{18}O$ to isolate changes in sea surface salinity (SSS). Before 4.5 Ma, $SST_{Mg/Ca}$ and SSS show moderate fluctuations, indicating a free exchange of surface ocean water masses between the Pacific and the Atlantic. The increase in $\delta^{18}O$ after 4.5 Ma represents increasing salinities in the Caribbean due to the

progressive closure of the Panamanian Gateway. The increase in Mg/Ca toward values of maximum 7 mmol/mol suggests that secondary influences have played a significant role. Evidence of crystalline overgrowths on the foraminiferal tests in correlation with aragonite, Sr/Ca, and productivity cyclicities indicates a diagenetic overprint on the foraminiferal tests. Laser ablation inductively coupled plasma–mass spectrometry analyses, however, do not show significantly increased Mg/Ca ratios in the crystalline overgrowths, and neither do calculations based on pore water data conclusively result in significantly elevated Mg/Ca ratios in the crystalline overgrowths. Alternatively, the elevated Mg/Ca ratios might have been caused by salinity as the $\delta^{18}$O record of Site 1000 has been interpreted to represent large fluctuations in SSS, and cultivating experiments have shown an increase in Mg/Ca with increasing salinity. We conclude that the Mg/Ca record <4.5 Ma can only reliably be considered for paleoceanographical purposes when the minimum values, not showing any evidence of secondary influences, are used, resulting in a warming of central Caribbean surface water masses after 4.5 Ma of ~2°C.

**Components:** 12,256 words, 8 figures, 5 tables.

**Keywords:** Mg/Ca paleothermometry; Panamanian Gateway; Pliocene; planktonic foraminifers.

**Index Terms:** 4999 Paleoceanography: General or miscellaneous; 3344 Atmospheric Processes: Paleoclimatology (0473, 4900); 1065 Geochemistry: Major and trace element geochemistry; 4954 Paleoceanography: Sea surface temperature.

**Received** 21 December 2006; **Revised** 27 August 2007; **Accepted** 5 October 2007; **Published** 12 January 2008.

Groeneveld, J., D. Nürnberg, R. Tiedemann, G.-J. Reichart, S. Steph, L. Reuning, D. Crudeli, and P. Mason (2008), Foraminiferal Mg/Ca increase in the Caribbean during the Pliocene: Western Atlantic Warm Pool formation, salinity influence, or diagenetic overprint?, *Geochem. Geophys. Geosyst.*, *9*, Q01P23, doi:10.1029/2006GC001564.

**Theme:** Development of the Foraminiferal Mg/Ca Proxy for Paleoceanography
**Guest Editor:** Pamela Martin

## 1. Introduction

### 1.1. Closure of the Panamanian Gateway

[2] The late Miocene/early Pliocene gradual closure of the Panamanian Gateway effectively changed oceanographic patterns between the Pacific and Atlantic oceans, and thus led to profound changes in global atmospheric circulation and climate. The closure of this ocean gateway was responsible for changing the Pacific, Caribbean, and Atlantic water mass signatures, generating the Western Atlantic Warm Pool (WAWP), and intensifying thermohaline circulation in the North Atlantic via increasing salt and heat transport to high northern latitudes [*Maier-Reimer et al.*, 1990; *Tiedemann and Franz*, 1997; *Haug and Tiedemann*, 1998; *Billups et al.*, 1999; *Haug et al.*, 2001]. As a consequence, the intensification of the Gulf Stream system might have had an important role in the initiation of the northern hemisphere glaciation (NHG), which started during the mid Pliocene [*Haug and Tiedemann*, 1998; *Driscoll and Haug*, 1998].

[3] *Haug et al.* [2001] interpreted the divergent pattern of planktonic $\delta^{18}$O records from the Caribbean (Site 999) and the tropical Pacific (Site 851) at 4.6 Ma and the subsequent 0.5‰ increase in $\delta^{18}$O in the Caribbean since ~4.2 Ma as the establishment of the salinity contrast between Pacific and Caribbean surface waters [*Keigwin*, 1982]. This hydrographic change was caused by the plate tectonic shoaling of the Panamanian sill to a water depth less than 100 m, which effectively restricted the water exchange between the Pacific and the Atlantic, and therefore increased SSS in the Caribbean by 1-2 salinity units by means of an increased atmospheric transport of water vapor from the Caribbean into the Pacific. Recent results from Caribbean Site 1000 [*Steph et al.*, 2006] show that, in accordance with this general increase in Caribbean SSS, salinity gradients within the Caribbean increased and varied on precessional timescales after 4.5 Ma. Low SSS gradients occurred during minima in northern hemisphere summer insolation and were interpreted to reflect enhanced inflow of low-salinity Pacific surface water into the Caribbean. During maxima in northern hemisphere

summer insolation, the inflow of low-salinity Pacific surface waters was reduced. In the northern Caribbean (Site 1000), higher-saline Atlantic water predominated, leading to a pronounced SSS gradient between the southern (Site 999) and northern Caribbean (Site 1000).

[4] The final closure of the Panamanian Gateway was not established until ~2.7–2.2 Ma, when the major exchange of mammals via the isthmus between North and South America took place [*Stehli and Webb*, 1985; *Webb*, 1997], and both nannofossil assemblages and $SST_{Mg/Ca}$ from the Caribbean and the eastern Pacific permanently diverged [*Kameo and Sato*, 2000; *Groeneveld et al.*, 2006].

## 1.2. Mg/Ca Paleothermometry

[5] The advantage of measuring Mg/Ca and $\delta^{18}O$ on the same biotic carrier is that synchronous estimates of SST and global ice volume can be determined and used to calculate $\delta^{18}O_{seawater}$, a proxy for SSS, thereby avoiding the bias of seasonality and/or habitat differences that occur when proxy data from different faunal groups are used.

[6] Commonly, the $\delta^{18}O$ signal of planktonic foraminifers records the combined effects of global ice volume, sea surface temperature, and local salinity. The Mg/Ca ratio of foraminiferal tests is mainly dependant on the temperature of the water in which the foraminifer calcifies as deduced from cultivating work and field studies [e.g., *Nürnberg*, 1995, 2000; *Nürnberg et al.*, 1996, 2000; *Lea et al.*, 1999; *Mashiotta et al.*, 1999; *Elderfield and Ganssen*, 2000; *Dekens et al.*, 2002]. Mg/Ca paleothermometry has hence become a widely applied tool in paleoceanography for the reconstruction of SSTs. Other factors like salinity [*Nürnberg et al.*, 1996; *Lea et al.*, 1999] and pH [*Lea et al.*, 1999] additionally affect foraminiferal Mg/Ca, but were hitherto considered to play minor roles as the absolute changes were considered to have been small [*Lea et al.*, 2000; *Nürnberg et al.*, 2000].

[7] The application of Mg/Ca paleothermometry to Pliocene sample material requires consideration of possible changes in the oceanic magnesium budget ($Mg/Ca_{seawater}$) [*Lear et al.*, 2000; *Billups and Schrag*, 2003; *Tripati et al.*, 2003]. Due to the long residence times of Mg (~13 m.y.) and Ca (~1.1 m.y.) in seawater [*Broecker and Peng*, 1982], paleo-SST reconstructions on short timescales are not affected by a change in $Mg/Ca_{seawater}$. Instead, on longer timescales Mg and Ca in seawater might have changed due to varying continental weathering rates [*Berner et al.*, 1983; *Wilkinson and Algeo*, 1989], hydrothermal alteration of basalt at mid ocean ridges [*Mottle and Wheat*, 1994; *Elderfield and Schultz*, 1996], carbonate deposition [*Wilkinson and Algeo*, 1989], and ion exchange reactions of Mg with clays [*Gieskes and Lawrence*, 1981]. On the basis of the models of *Wilkinson and Algeo* [1989] and *Stanley and Hardie* [1998], $Mg/Ca_{seawater}$ was lowered by ~0.4 mol/mol during the early Pliocene. From cultivating experiments *Brown* [1996] concluded that $Mg/Ca_{foram}$ is linearly dependant on $Mg/Ca_{solution}$ (0.1 mol/mol change in $Mg/Ca_{seawater}$ leads to 0.059 mmol/mol change in $Mg/Ca_{foram}$). Also, *Ries* [2004] showed that several carbonate building organisms exhibit a close relationship between $Mg/Ca_{biotic\ calcite}$ and $Mg/Ca_{solution}$. Correction of the Mg/Ca record of Site 1000 by applying the formula of *Lear et al.* [2000] results in a constant offset of the $SST_{Mg/Ca}$ record toward higher temperatures by ~1°C (Figure 3 in section 3). As a correction for this change in $Mg/Ca_{seawater}$ is not routinely applied in other published high-resolution Mg/Ca records of the Pliocene [*Wara et al.*, 2005; *Bartoli et al.*, 2005; *Groeneveld et al.*, 2006] we did not further include this correction into our discussion.

[8] Experiments with electron microprobe have shown that Mg/Ca ratios within single foraminiferal tests are heterogeneously distributed [*Nürnberg*, 1995; *Nürnberg et al.*, 1996; *Brown and Elderfield*, 1996; *McKenna and Prell*, 2004; *Sadekov et al.*, 2005]. Recent studies used laser ablation inductively coupled plasma–mass spectrometry (LA-ICP-MS) to further reveal intertest and intratest variability [*Reichart et al.*, 2003; *Hathorne et al.*, 2003; *Eggins et al.*, 2003; *Pena et al.*, 2005]. Here, we used the advantage of high-resolution analyses through foraminiferal tests to detect and quantify the possible influence of contaminant phases on the primary calcite [*Reichart et al.*, 2003; *Pena et al.*, 2005].

[9] We present a high-resolution Mg/Ca record for ODP Site 1000 from the Caribbean for the time interval from 5.6 Ma to 3.9 Ma for the planktonic foraminifer *G. sacculifer*. The main objectives of the study were (1) to investigate the development of Caribbean SST with the restriction of the exchange of upper ocean water masses between the Pacific and the Caribbean, due to the progressive closure of the Panamanian Gateway, and (2) to

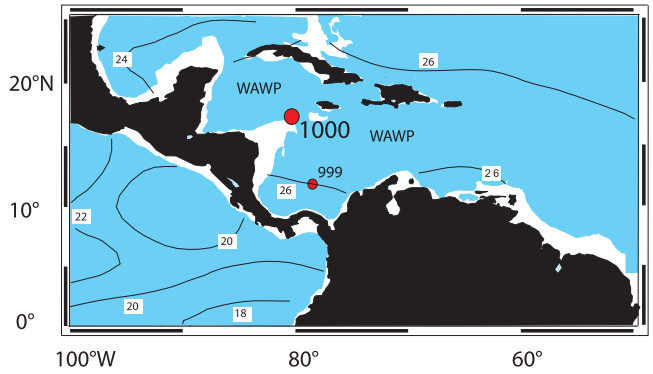


**Figure 1.** Present-day configuration of the Caribbean Sea with the location of Site 1000 (16°33′N, 79°52′W, 916 m water depth). Also indicated is Site 999 (12°44′N, 78°44′W, 2828 m water depth) [*Haug et al.*, 2001]. WAWP is the Western Atlantic Warm Pool. Isolines indicate annual average temperatures at a water depth of ~50 m [*Levitus and Boyer*, 1994], the assumed habitat depth of *G. sacculifer*.

explore the potential influence of secondary effects, i.e., diagenesis and salinity, on the Mg/Ca.

## 2. Material and Methods

[10] ODP Site 1000 was cored during Leg 165 on the Nicaraguan Rise (Pedro Channel) in the Caribbean Sea (16°33.222′N, 79°52.044′W, Figure 1). The shallow site location of 916 m in comparison with the depth of the Caribbean lysocline at 4000 m [*Archer*, 1996] implies that carbonate dissolution is negligible. Samples were taken every 10 cm, reflecting a temporal resolution of ~3 ka per sample. The age model for Site 1000 is based on the $\delta^{18}$O record of the benthic foraminifer *Cibicidoides wuellerstorfi* [*Steph et al.*, 2006]. Since no composite depth existed for Site 1000, a preliminary age model was constructed by identifying major isotopic stages according to the nomenclature of *Shackleton et al.* [1995]. The preliminary age model was then correlated to the orbitally tuned age model of ODP Site 925/926 from Ceara Rise [*Bickert et al.*, 1997; *Tiedemann and Franz*, 1997; *Shackleton and Hall*, 1997]. The final age model revealed the presence of dominant precession cycles in the planktonic $\delta^{18}$O record, which were then used to orbitally tune the age model [*Steph et al.*, 2006].

### 2.1. Mg/Ca Analysis

[11] Twenty to twenty-five specimens of *Globigerinoides sacculifer* were selected from the 315–400 $\mu$m size fraction. Specimens visibly contaminated by ferromanganese oxides and specimens with a final sac-like chamber were not selected for analysis. After gentle crushing, the foraminiferal tests were cleaned according to the cleaning protocol of *Barker et al.* [2003]. To remove clays, the samples were rinsed 4–6 times with distilled deionized water and twice with methanol (suprapure) with ultrasonical cleaning steps (2–3 minutes) after each rinse. Subsequently, samples were treated with a hot (97°C) oxidizing 1% NaOH/$H_2O_2$ solution (10 mL 0.1 M NaOH (analytical grade); 100 $\mu$L 30% $H_2O_2$ (suprapur)) for 10 minutes to remove organic matter. Every 2.5 minutes, the vials were rapped on the bench top to release any gaseous buildup. After 5 minutes, the samples were placed in an ultrasonic bath for a few seconds in order to maintain contact between reagent and sample. This treatment was repeated after refreshment of the oxidizing solution. Any remaining oxidizing solution was removed by three rinsing steps with distilled deionized water. After transferring the samples into clean vials, a weak acid leach with 250 $\mu$L 0.001 M $HNO_3$ (subboiled distilled) was applied with 30 seconds ultrasonic treatment and subsequent two rinses with distilled deionized water. After cleaning, the samples were dissolved in 0.075 M nitric acid ($HNO_3$) (subboiled distilled) and diluted with distilled deionized water up to 3 mL containing 10 ppm of yttrium as an internal standard.

[12] Analyses were run on an ICP-OES (ISA Jobin Yvon, Spex Instruments S.A. GmbH) with polychromator applying yttrium as an internal standard. We selected element lines for analyses which were most intensive and undisturbed (Ca: 317.93 nm; Mg: 279.55 nm; Sr: 407.77 nm; Fe: 238.21 nm; Mn: 257.61 nm; and Y: 371.03 nm). Element detection was performed with photomultipliers, the high tension of which was adapted to each

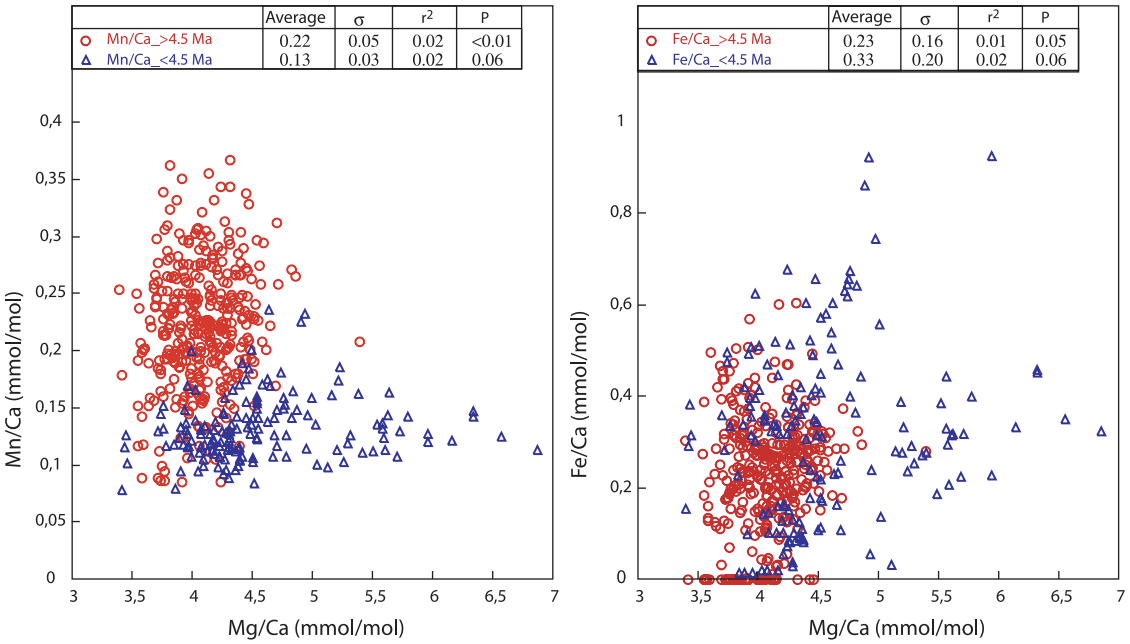


**Figure 2.** Mn/Ca and Fe/Ca results of Site 1000 in comparison with Mg/Ca for the time intervals before and after 4.5 Ma. The absence of a correlation between Mn/Ca and Mg/Ca indicates that possible Mn carbonates have no influence on Mg/Ca. The absence of a correlation between Fe/Ca and Mg/Ca indicates that no clay minerals remain after the cleaning process.

element concentration range. The relative standard deviation for the analysis of magnesium was 0.45% and for calcium 0.15%. The Mg/Ca reproducibility of replicate samples (n = 22) of *G. sacculifer* is 3.3% ($\sigma$ = 0.104), giving a temperature error of ±0.7°C. The conversion of foraminiferal Mg/Ca ratios into $SST_{Mg/Ca}$ was carried out by applying the equation of *Nürnberg et al.* [2000] (SST = ((Log (Mg/Ca)-Log 0.491)/0.033). The total error on paleotemperatures reconstructed by means of Mg/Ca is 1–1.5°C [*Nürnberg et al.*, 2000; *Lea et al.*, 1999].

[13] We used an artificial solution, comparable to our calibration standards, to monitor the quality of our Mg/Ca measurements with a Mg/Ca ratio of 2.90 mmol/mol as in-house standard. The long-term standard deviation of this standard is 0.026 mmol/mol or 0.91%. Interlaboratory comparison was done by measuring a set of standards provided by M. Greaves (University of Cambridge) [*Greaves et al.*, 2005]. On average, our ICP-OES measurements were 0.5% (~0.02 mmol/mol) lower than those from the Cambridge laboratory, which is within the error range given by *Rosenthal et al.* [2004].

[14] Several samples, which partly exhibited crystalline overgrowths and which were selected for SEM and laser ablation analysis, were also cleaned by including the reductive cleaning step described by *Boyle and Keigwin* [1985]. Mg/Ca ratios of these samples were systematically lower by 0.37 mmol/mol (range 0.26–0.48 mmol/mol) than those cleaned without the reduction step. This offset is comparable to the offset between the "Mg method" and the "Cd method" as shown by *Rosenthal et al.* [2004].

[15] Iron and manganese concentrations were monitored to identify contaminant clay particles and manganese-rich carbonate coatings, which might affect the foraminiferal Mg/Ca ratios [*Boyle*, 1983; *Barker et al.*, 2003]. Samples older than 4.5 Ma show average Fe/Ca ratios of 0.23 mmol/mol ($\sigma$ = 0.16) and average Mn/Ca ratios of 0.22 mmol/mol ($\sigma$ = 0.05) (Figure 2). Although these values are higher than the 0.1 mmol/mol Mn/Ca and Fe/Ca ratios given by *Barker et al.* [2003] for clean, uncontaminated foraminiferal tests, we assume our Mg/Ca analyses unaffected by contamination as no correlation with Mg/Ca exists for both Fe/Ca ($r^2$ = 0.01; Probability (P) = 0.05) and Mn/Ca ($r^2$ = 0.02; P = <0.01) (Figure 2). For samples younger than 4.5 Ma, average Fe/Ca ratios are 0.33 mmol/mol ($\sigma$ = 0.20) and average Mn/Ca ratios are 0.13 ($\sigma$ = 0.03), and lack any correlation with Mg/Ca ($r^2$ = 0.02; P = 0.06 for Mg/Ca versus Fe/Ca, $r^2$ = 0.02; P = 0.06 for Mg/Ca versus Mn/Ca)

**Table 1.** Comparison Between Bulk ICP-OES Measurements and LA-ICP-MS Analyses for Mg/Ca and Sr/Ca[a]

| Sample | Age, Ma | State | Number of Profiles (Analyses/Profile) | Mg/Ca, mmol/mol, ICP-OES | Mg/Ca uncont.interval, mmol/mol, LA-ICP-MS1 | Sr/Ca, mmol/mol, ICP-OES | Mg/Ca uncont.interval, mmol/mol, LA-ICP-MS[b] |
|---|---|---|---|---|---|---|---|
| 1000,14-5-95 | 3.952 | no crystalline overgrowth | 4 (37) | 4.30 | 3.84 | 1.39 | 1.45 |
| 1000,14-5-145 | 3.965 | no crystalline overgrowth | 4 (38) | 4.39 | 4.29 | 1.38 | 1.44 |
| 1000,14-5-115 | 3.958 | crystalline overgrowth | 5 (45) | 6.57 | 6.89 | 1.58 | 1.66 |
| 1000,14-5-125 | 3.960 | crystalline overgrowth | 4 (47) | 6.87 | 6.23 | 1.54 | 1.55 |

[a] Average results are shown from multiple ablation profiles through cleaned *G. sacculifer* tests from two contaminated, with crystalline overgrowths, samples (14-5-115 and 14-5-125) and two uncontaminated, without crystalline overgrowths, samples (14-5-95 and 14-5-145). The calculated Mg/Ca ratios derived from the LA-ICP-MS measurements agree, within the method standard deviation of 5–10%, to the whole-test ICP-OES measurements performed on the same samples.
[b] Relative standard deviation is 5–10%.

(Figure 2). Samples from which Fe/Ca and Mn/Ca ratios were more than $2\sigma$ higher than the average were reanalyzed.

## 2.2. LA-ICP-MS

[16] Laser ablation inductively coupled plasma–mass spectrometry (LA-ICP-MS) (ICP-MS, Micromass Platform) was used to measure high-resolution Mg, Sr and Ca chamber wall profiles of selected foraminiferal tests. For the laser ablation measurements we selected cleaned *G. sacculifer* fragments from four different samples, two samples with crystalline overgrowths (sample 14-5-115 and sample 14-5-125) and two samples without crystalline overgrowths (sample 14-5-95 and sample 14-5-145) (Table 1). The fragments were cleaned according to the protocol described in paragraph 2.1. Multiple laser ablation profiles were ablated in different foraminiferal fragments from the same sample to elucidate in-test heterogeneities. In total, 25 profiles were ablated, 11 from foraminiferal test fragments without crystalline overgrowths, and 14 from fragments with crystalline overgrowths (Table 1).

[17] Using an Excimer 193 nm deep ultra violet laser (Lambda Physik) with Geolas optics [*Günther et al.*, 1997] craters of 80 $\mu$m were ablated during the analyses. Energy density at the sample surface was kept at 2 mJ/cm$^2$, shot repetition rate at 8 Hz. Laser ablation of calcite requires ablation at ultra violet wavelengths since higher wavelengths result in uncontrolled cleavage. The ablated material was transported on a continuous He flow and mixed with an Ar make up gas before injection into the Ar plasma of the quadrupole ICP-MS instrument (Micromass Platform). A collision and reaction cell was used to improve results by reducing spectral interferences on the minor isotopes of Ca ($^{42}$Ca, $^{43}$Ca and $^{44}$Ca). Interelemental fractionation was insignificant due to the relative low depth to width ratio of the ablation craters produced [*Mason and Mank*, 2001]. The use of a collision cell also prevented interference of clusters like $^{12}C^{16}O^{16}O$. Although the Excimer UV-193 usually does not show any matrix effects, possible matrix effects were nevertheless checked with an in-house matrix matched standard (Utrecht Calcite). Calibration was performed against U.S. National Institute of Standards and Technology SRM 612 glass using the concentration data of *Pearce et al.* [1997], with Ca as an internal standard. Calcium carbonate is well suited for LA-ICP-MS because Ca can be used as an internal standard at 40 wt%. For quantifying Ca we used mass 44, while monitoring masses 42 and 43 as an internal check. Using Ca as an internal standard allows direct comparison to trace metal to Ca ratios from traditional wet-chemical studies. Magnesium concentrations were calculated using masses 24 and 26. Although the accuracy for the more abundant mass 24 is higher, both isotopes agree within a few percent. For calculating strontium concentrations mass 88 was used. Analyses were performed at the Faculty of Geosciences, Utrecht University, Netherlands.

[18] With initiation of the ablation process preferential ablation of material from surfaces that lie orthogonal to the incident laser beam results in greater ablation from the tops of interpore ridges and spine bases [*Eggins et al.*, 2003]. This means that the ablation crater is not flat but follows the

curvature of the foraminiferal test and therefore should reveal elevated element concentrations in a diagenetic coating when present. Further in the ablation process the craters become increasingly flatter bottomed. This results in a smoothing of the signal when the ablation reaches the pores on the other side of the test. The fragments of each sample were measured both from the inner side toward the outer side and the other way around to certify that no smoothing of a possible coating peak occurred.

### 2.3. Analysis of $\delta^{18}O$

[19] For stable isotope analysis 10 specimens of *G. sacculifer* (without sac-like final chamber) were picked from the 315–400 $\mu$m size fraction. All isotope analyses were run at IFM-GEOMAR (Kiel) on a Finnigan MAT 252 Delta-Plus Advantage Mass Spectrometer equipped with an automated Kiel Carbonate Preparation line. The mass spectrometer is calibrated to NBS 19, and the isotope values are reported in ‰ relative to the VPDB (Vienna PDB) scale. The external reproducibility of in-house carbonate standards was ±0.08‰ (±1$\sigma$) for $\delta^{18}O$ [*Steph et al.*, 2006].

### 2.4. Carbonate Mineralogy

[20] Carbonate mineralogy was determined using the Philips PW1710 diffractometer at IFM-Geomar with a cobalt K$\sigma$ tube at 40 KV and 35 mA. For the interval 4.1 to 3.8 Ma, one sample per 10 cm was analyzed. Samples older than 4.1 Ma were analyzed with a spacing of 30 cm. The samples were scanned from 25°–40° at a scanning speed of 0.01 steps per second to cover the significant peaks of the various carbonate minerals. The percentage of aragonite and calcite relative to total carbonate content was calculated from peak area ratios using in-house calibration curves. Peak areas were measured using the computer-based integration program MacDiff (R. Petschick, Johann Wolfgang von Goethe-Universität, Frankfurt am Main, Germany, 1999). The standard deviation (1$\sigma$) of this method, calculated from replicates, is 1%. The nonlinear relationship between calcite and aragonite was calculated from ratios calibrated from standards measured on the diffractometer.

### 2.5. Calcareous Nannofossil Analysis

[21] The relative abundance record of the coccolithophorid *Florisphaera profunda* was used as a proxy to reconstruct variations in primary productivity by means of high-resolution scanning electron microscope (SEM) analysis [*Crudeli*, 2005]. Sample resolution was the same as for Mg/Ca and $\delta^{18}O$. According to *Crudeli and Kinkel* [2004], 0.1 g of dry sediment was diluted with carbonate-saturated tap water. The solution was then divided with a rotary splitter device. A final solution with 0.001 g of sediment was filtered with a low-pressure vacuum pump onto a polycarbonate-membrane filter (pore size: 0.40 $\mu$m; diameter: 50 mm). A segment of the filter was then mounted on a scanning electron microscope (SEM) stub. SEM analyses were conducted at a magnification of 6000X using a CamScan 44-Serie-2-CS-44 SEM (University of Kiel).

## 3. Results and Discussion

[22] The range of Mg/Ca ratios in *G. sacculifer* from Site 1000 can be divided into two time intervals, before and after 4.5 Ma (Figure 3). Before 4.5 Ma, Mg/Ca ratios range between 3.5 and 4.5 mmol/mol, translating into $SST_{Mg/Ca}$ between 26.5°C and 29°C. After 4.5 Ma, the range of Mg/Ca ratios increases to values between 4 and 7 mmol/mol, providing $SST_{Mg/Ca}$ between 28°C and 35°C (Figure 3).

### 3.1. Free Exchange of Upper Ocean Water Masses Before 4.5 Ma

[23] The latest Miocene to earliest Pliocene time interval (5.6–4.5 Ma) is characterized by the absence of an explicit correlation between Mg/Ca and $\delta^{18}O$ ($r^2$ = <0.01; P = 0.39). The $\delta^{18}O$ record shows moderate variation, ranging between −1.05‰ and −1.7‰. A pronounced salinity effect on planktonic $\delta^{18}O$ can be excluded for this time interval, as the free exchange between Pacific and Caribbean surface water masses prohibited the establishment of salinity gradients [*Haug et al.*, 2001]. Hence the fluctuations in $\delta^{18}O$ are interpreted to reflect changes in global ice volume and in SST. Orbital-scale changes in global ice volume affected the late Miocene/early Pliocene $\delta^{18}O$ signal by up to 0.15–0.25‰ [*Hodell and Warnke*, 1991; *Kennett and Hodell*, 1993; *Tiedemann et al.*, 1994; *Shackleton et al.*, 1995; *Mix et al.*, 1995], while variations in SST were 2–3°C as indicated by the Mg/Ca record.

### 3.2. Progressive Restriction of Upper Ocean Water Masses After 4.5 Ma

[24] After 4.5 Ma, we observe an overall positive correlation between the Mg/Ca and $\delta^{18}O$ records of *G. sacculifer* ($r^2$ = 0.48; P = <0.0001) (Figure 3).

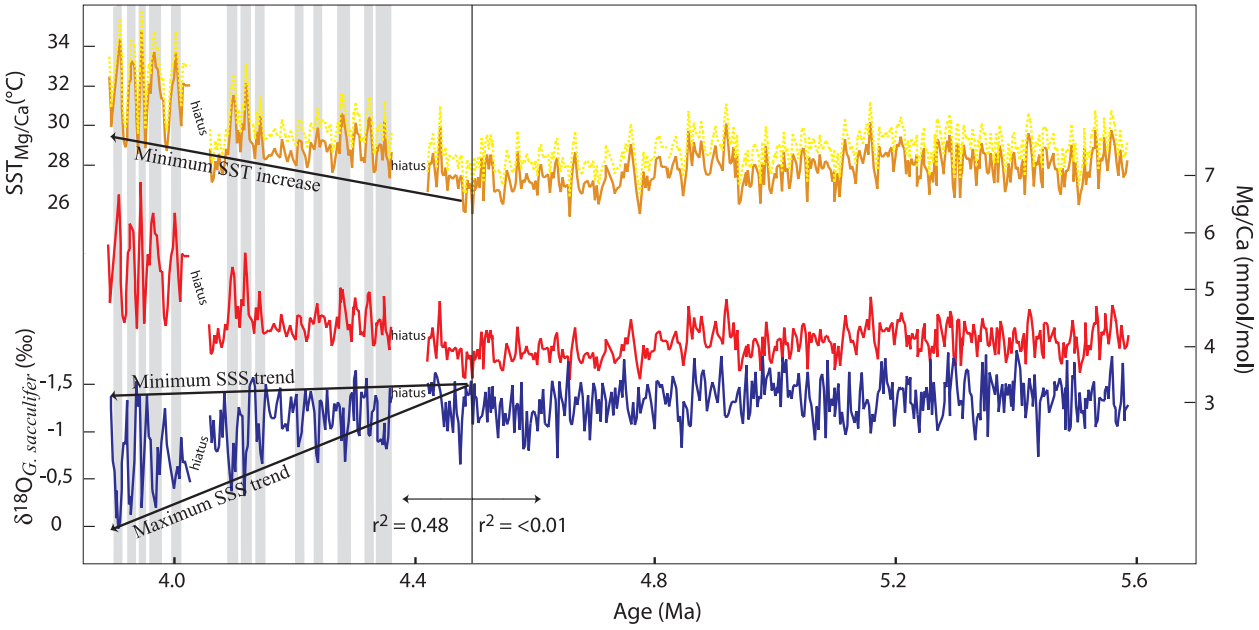


**Figure 3.** Results for Site 1000 for the time interval 5.6 Ma to 3.9 Ma. Arrow in Mg/Ca indicates the paleoceanographically reliable trend, solely based on those samples which do not contain any indications for secondary influences on Mg/Ca, associated with the restriction of upper ocean water masses between the Pacific and the Caribbean since 4.5 Ma. The two arrows in $\delta^{18}O$ represent the paleoceanographically interpreted increase in salinity (following maximum values) and the trend which was established for the unaffected Mg/Ca samples (minimum trend). Mg/Ca ratios are measured on tests of the planktonic foraminifer *G. sacculifer*. Mg/Ca ratios are converted into SSTs using the formula of *Nürnberg et al.*, [2000]. Dashed line represents $SST_{Mg/Ca}$ when a correction for the $Mg/Ca_{seawater}$ for the Pliocene is applied. $\delta^{18}O$ was measured on tests of the planktonic foraminifer *G. sacculifer* [*Steph et al.*, 2006]. Bars show the positive correlation between Mg/Ca and $\delta^{18}O$. Note that $\delta^{18}O$ is plotted in reverse.

Such a distinct positive correlation was hitherto not described. The Mg/Ca ratios suggest $SST_{Mg/Ca}$ of maximum 35°C and amplitudes of up to 5°C (Figure 3), with a general warming trend of 4°C between 4.5 Ma and 3.9 Ma. $\delta^{18}O$ values range between −1.6‰ and 0‰, show increasing amplitudes up to 1.4‰, and show a general trend toward higher values [*Steph et al.*, 2006].

[25] The extreme $SST_{Mg/Ca}$ maxima of up to 35°C and amplitudes of up to 5°C appear to be very unlikely for the early Pliocene. Firstly, modern SSTs at ~30–50 m water depth, the assumed habitat depth of *G. sacculifer* [*Fairbanks et al.*, 1982], do not exceed 30–31°C in open ocean conditions [*Levitus and Boyer*, 1994], and it is unreasonable to expect significantly higher SSTs during the early Pliocene. Maximum SSTs during the course of El Niño, for example, never reach much beyond 29°C [*Philander*, 1990]. Several mechanisms have been described as contributing to this stability of tropical SSTs like cloud albedo effects, evaporation, characteristics of dry-air pools, and heat transport out of the tropics [*Newell*, 1979; *Ramanathan and Collins*, 1991; *Waliser and Graham*, 1993; *Pierrehumbert*, 1995]. Secondly, this early Pliocene time interval is known to represent a globally warm and stable climate of unipolar glaciation with a pole-equator temperature gradient which was smaller than today [*Cronin et al.*, 1993; *Crowley*, 1996]. In addition, studies in the high-latitudinal Atlantic indicated that SSTs might have been warmer by up to 8°C than today, while the tropical SSTs remained the same or were, due to increased heat transport to higher latitudes, even slightly cooler than today [*Cronin et al.*, 1993; *Crowley*, 1996; *Dowsett et al.*, 1996; *Billups et al.*, 1998; *Groeneveld et al.*, 2006]. Hence amplitudes in $SST_{Mg/Ca}$ as large as 5°C appear to be rather unlikely.

[26] How do we then explain the extremely high $SST_{Mg/Ca,}$ the large $SST_{Mg/Ca}$ amplitude variations, and the positive correlation with $\delta^{18}O$ during the time interval 4.5–3.9 Ma? In the following sections we discussed two potential tracts, diagenetic

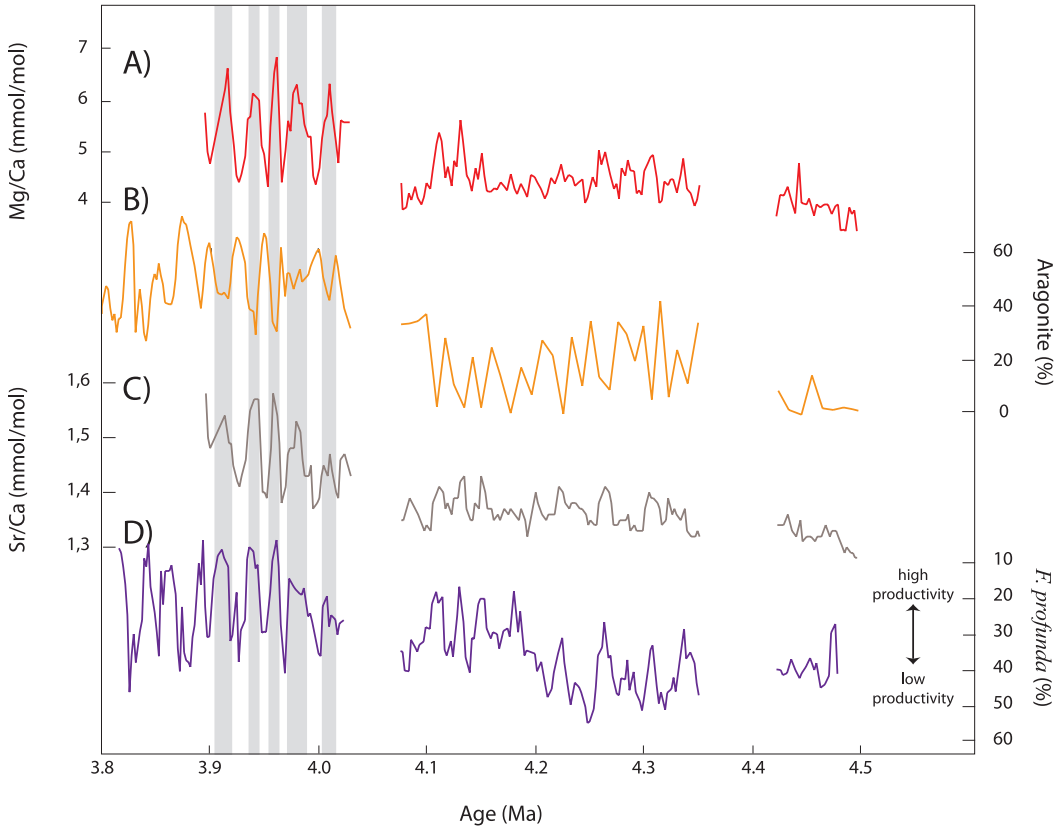


**Figure 4.** Mg/Ca results in comparison with aragonite content, $Sr/Ca_{G.\ sacculifer}$, and relative abundance of *F. profunda* for the time interval from 4.5 Ma to 3.9 Ma for Site 1000. Bars show the correlation between the individual records. (a) Mg/Ca ratios, measured on tests of the planktonic foraminifer *G. sacculifer.* (b) Aragonite content, measured on bulk sediment by a Philips PW1710 diffractometer. (c) Sr/Ca ratios, measured on tests of the planktonic foraminifer *G. sacculifer*, indicative of diagenetic alteration. (d) Relative abundance (plotted in reverse) of *F. profunda*, indicative of variation in primary productivity.

overprint (section 4) and salinity influence (section 5), of explaining the anomalous Mg/Ca signal.

## 4. Diagenetic Alteration of Foraminiferal Tests After 4.5 Ma

[27] Sediments with high calcium carbonate contents are prone to diagenetic overprinting, dissolution and reprecipitation, especially when the carbonate is present as metastable aragonite or high-Mg calcite [*Swart and Guzikowski*, 1988; *Malone et al.*, 1990; *Munnecke et al.*, 1997; *Melim et al.*, 2002]. Site 1000 is surrounded by carbonate platforms which can supply large amounts of aragonite to the core location [*Sigurdsson et al.*, 1997]. Since aragonite in sediments is susceptible to dissolution, reprecipitation as inorganic calcite can subsequently occur. After 4.5 Ma alternations between aragonite-rich (up to 60%) and nodular, aragonite-poor layers (<30%) occur, showing precessional cyclicity (Figure 4).

[28] Relative abundance variations in the coccolithophorid *Florisphaera profunda* at Site 1000 reflect temporal changes in marine productivity (Figure 4), with low abundances during times of higher marine productivity at the surface of the mixed layer [*Molfino and McIntyre*, 1990; *Beaufort et al.*, 1997; *de Garidel-Thoron et al.*, 2001]. Higher marine productivity enhances nutrient utilization, reduces nutrient flux to the bottom of the photic zone, and hence reduces the relative abundances of *F. profunda* [*Crudeli*, 2005]. The abundance variations of *F. profunda* are positively correlated with the aragonite record ($r^2 = 0.50$) (Figure 4), implying that at times of enhanced marine productivity, more organic matter is decomposed, thereby lowering the pore water pH, favoring aragonite dissolution, and subsequently

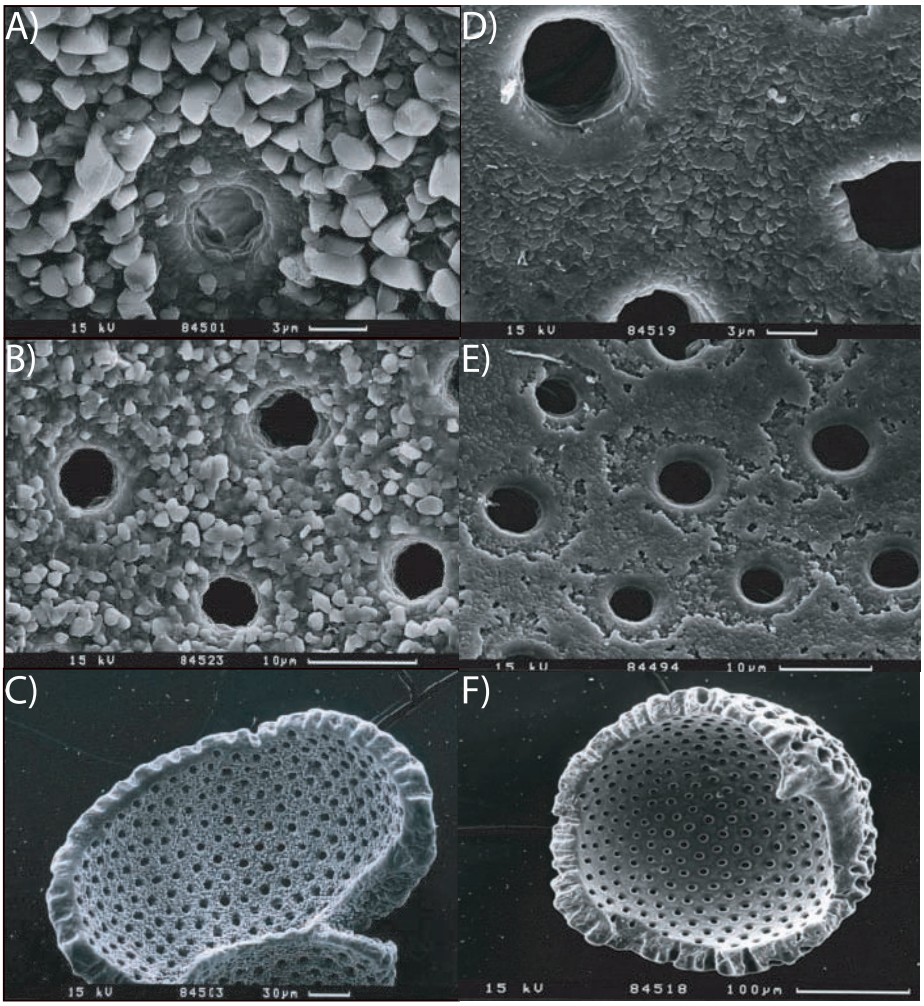


**Figure 5.** Scanning electron microscope images (CAMSCAN-Serie-2-CS-44, University of Kiel, Germany) of cleaned tests of the planktonic foraminifer *G. sacculifer* of Site 1000. Bars indicate the scale of the images. For comparison, pairs of photos of about the same size scale are plotted together, one from a contaminated test and one from an uncontaminated test. (a–c) Foraminiferal tests containing an overgrowth of diagenetic crystals. (d–f) Cleaned foraminiferal tests without the presence of diagenetic crystals. Slight indications of dissolution are visible, most likely caused by the intense cleaning procedure.

inducing reprecipitation as inorganic calcite [*Dix and Mullins*, 1992; *Frank and Bernet*, 2000].

[29] Additionally, SEM analyses show that after 4.5 Ma the inner surfaces of tests of *G. sacculifer* are regularly covered by crystalline overgrowths, which are resilient to the cleaning procedures routinely applied before Mg/Ca analyses (Figures 5a–5c). The size of the single crystals amounts to 2–3 $\mu$m. Thus the alternating cycles of relative abundance of *F. profunda* and aragonite in combination with the SEM analyses show that a diagenetic overprint is present in these samples. Whether the diagenetic overprint has a significant influence on foraminiferal $\delta^{18}$O and Mg/Ca is discussed in sections 4.1 and 4.2.

### 4.1. Assessing the Diagenetic Influence on $\delta^{18}$O

[30] The positive correlation between $\delta^{18}$O, aragonite, and the relative abundance of *F. profunda* after 4.5 Ma (Figures 3 and 4) implies that $\delta^{18}$O is possibly affected by carbonate diagenesis [*Killingley*, 1983; *Schrag et al.*, 1995; *Pearson et al.*, 2001]. The precipitation of diagenetic calcite from cold pore water alters the original $\delta^{18}$O values toward higher values. We compared the $\delta^{18}$O record of *G. sacculifer* of Site 1000 with the one from southwestern Caribbean Site 999 [*Haug et al.*, 2001; *Steph et al.*, 2006] to further assess the diagenetic imprint on precessional periods (Figure 6a). Site 999 (12°44′N, 78°44′W) is located in 2828 m water depth and

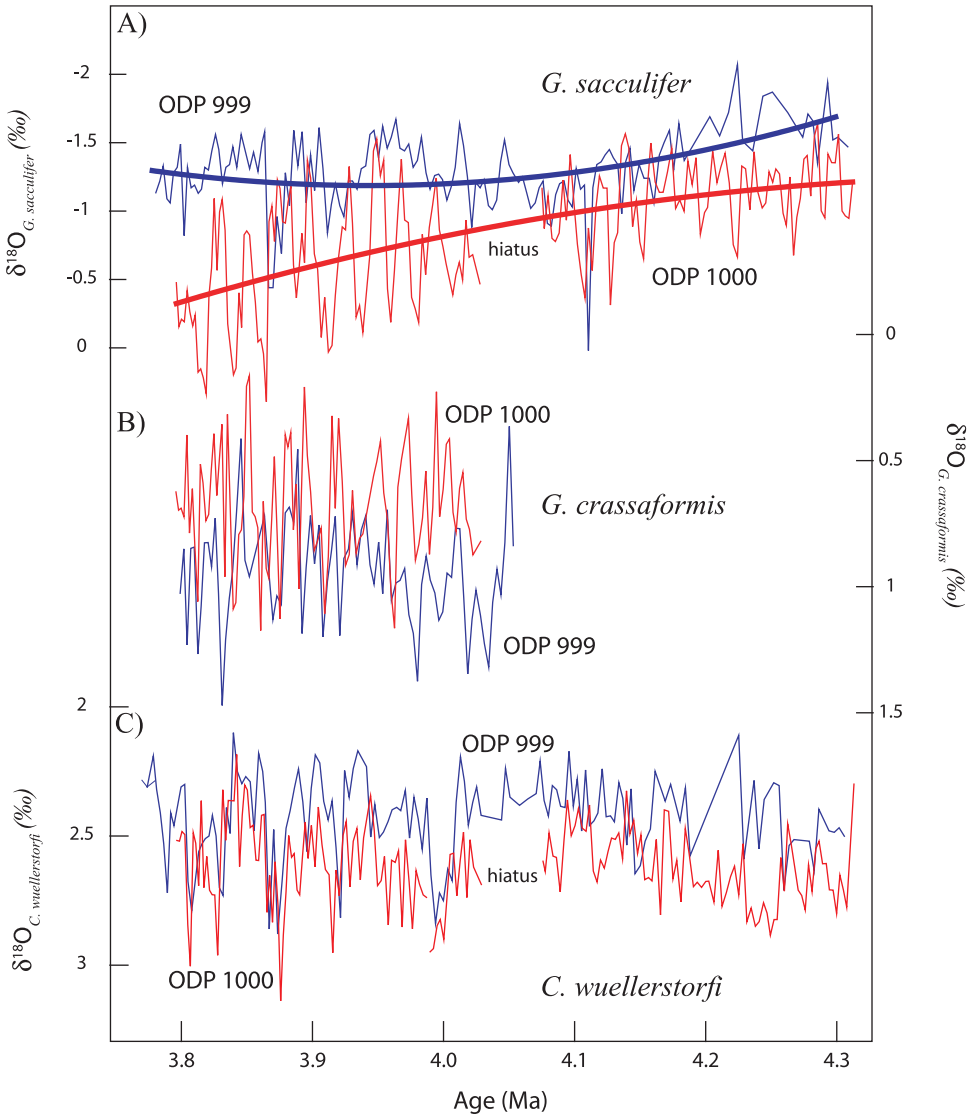


**Figure 6.** Comparison of $\delta^{18}O$ records for the planktonic foraminifers *G. sacculifer* and *G. crassaformis* and the benthic foraminifer *C. wuellerstorfi* between Site 1000 and southern Caribbean Site 999. (a) Comparison of *G. sacculifer* shows the absence of pronounced precession cycles at Site 999 as well as much smaller amplitudes than at Site 1000. This possibly points to a diagenetic imprint on the results of Site 1000. (b) Comparison of *G. crassaformis* shows much smaller amplitudes at both sites in comparison with the *G. sacculifer* record of Site 1000, arguing against a diagenetic overprint on the record of Site 1000. (c) Comparison of *C. wuellerstorfi* shows obliquity-related cyclicities at both Site 999 and Site 1000 instead of diagenetically induced precessional cyclicities, arguing against a diagenetic overprint on the record of Site 1000. The offset toward higher values at Site 999 is due to its deeper location and hence to a slightly lower bottom water temperature.

thus well below the aragonite compensation depth. The isotope curves from this site are used as reference records as diagenetic overprints on the $\delta^{18}O$ signal are considered to be negligible. The isotope fluctuations of *G. sacculifer* at Site 999 reveal no clear response to precession-induced climate variability, the amplitudes between 4.2 and 3.8 Ma are distinctly lower (~0.6‰ versus 1.3‰ at Site 1000), and the $\delta^{18}O$ trend toward higher values is less pronounced (Figure 6a). This suggests that a diagenetic overprint may have altered the $\delta^{18}O$ signal at Site 1000. Also, the cyclic variability of the $\delta^{18}O$ signal at Site 1000 is negatively correlated with the aragonite content. Crystalline overgrowths on foraminiferal tests are found only at samples where $\delta^{18}O$ values are high and aragonite contents are low.

[31] In addition to the $\delta^{18}O$ record of *G. sacculifer*, we measured $\delta^{18}O$ records of the deep dwelling planktonic foraminifer *Globorotalia crassaformis*, and the epibenthic foraminifer *Cibicidoides wuellerstorfi* at Sites 999 and 1000 [*Steph et al.*, 2006] for the interval from 4.1–3.8 Ma (Figure 6). The comparison of the $\delta^{18}O$ records of *G. crassaformis* and *C. wuellerstorfi* does not support the presence of a significant diagenetic overprint (Figure 6). *G. crassaformis* is a planktonic foraminiferal species with a deep calcification depth (250–500 m [*Niebler et al.*, 1999]). Accordingly, $\delta^{18}O$ values should increase with increasing habitat depth as temperature decreases. This pattern might be modified by changes in local $\delta^{18}O_{water}$. In contrast to the mixed layer, regional differences in subsurface water mass signatures (temperature and salinity) between Sites 999 and 1000 should be low at water depths of 250 to 500 m. We do not expect significant influence from the low-salinity Pacific inflow at these water depths, as the Panama sill was shallower than 100 m since 4.2 Ma [*Haug et al.*, 2001]. Accordingly, we would expect similar $\delta^{18}O$ values, amplitudes, and temporal variations for the deep dwelling *G. crassaformis* at both sites if diagenetic overprints were negligible. Indeed, the comparison of $\delta^{18}O$ records from *G. crassaformis* reflects similar $\delta^{18}O$ amplitudes (about 0.7‰) and temporal variations within the time interval from 4.1–3.8 Ma (Figure 6b) which are about 0.3‰ higher at Site 999. At Site 1000, the $\delta^{18}O$ amplitudes of *G. crassaformis* are only half the $\delta^{18}O$ amplitudes of *G. sacculifer* and the $\delta^{18}O$ variability of *G. crassaformis* at precessional periodicities is as weak as at Site 999. Assuming a strong diagenetic overprint, the $\delta^{18}O$ values should be higher at Site 1000 and the precessional amplitudes should be much higher. This is not the case and argues against significant diagenetic overprint on the $\delta^{18}O$ signal. The temporal variability of the benthic $\delta^{18}O$ records from Sites 999 and 1000 are similar, following a 41-ka rhythm with comparable amplitudes (Figure 6c). Again, a strong diagenetic overprint should have strengthened the cyclic variability at precessional periodicities which is not observed.

[32] The isotopic composition of the pore water is an additional factor which determines the composition of diagenetic calcite [*Killingley*, 1983; *Schrag et al.*, 1995]. As pore water measurements of $\delta^{18}O$ are not available for Site 1000, we used ODP Site 1006 from the Great Bahama Bank as analogue for Site 1000, as their respective settings are similar [*Reuning et al.*, 2005]. *Reuning et al.* [2005] used pore water measurements of $\delta^{18}O$ and varying recrystallization rates to explore the possible range of $\delta^{18}O$ values of diagenetic calcite in early Pliocene samples from Site 1006. They found that the impact of up to 5% recrystallization of the foraminiferal calcite did not have a significant effect (~0.1‰) on the primary signal. This suggests that, even though the $\delta^{18}O$ values of Site 1000 appear to have higher values than expected, this is not supported by the magnitude of the diagenetic overprint. However, if the diagenetic alteration of the tests is more extensive than just the visible crystalline overgrowth [*Pearson et al.*, 2001; *Hover et al.*, 2001], it cannot be excluded that the maximum $\delta^{18}O$ values of Site 1000 younger than 4.5 Ma are affected by a diagenetic overprint.

[33] We suggest that a significant diagenetic imprint on the $\delta^{18}O$ signal of *G. sacculifer*, without accompanying effects on the $\delta^{18}O$ variability of *G. crassaformis*, and *C. wuellerstorfi*, appears to be unlikely. Therefore we argue that, in agreement with *Steph et al.* [2006], the pronounced precession-related amplitudes within the $\delta^{18}O$ record of *G. sacculifer* mainly reflect changes in oceanography and hence represent large fluctuations in salinity.

## 4.2. Assessing the Diagenetic Influence on Mg/Ca

[34] The positive correlation between Mg/Ca, aragonite, and the relative abundance of *F. profunda* (Figure 4) and the presence of crystalline overgrowths on foraminiferal tests (Figures 5a–5c), suggests that diagenesis might be responsible for the anomalously high Mg/Ca ratios of up to 7 mmol/mol. Previous studies from the Little Bahama Bank showed planktonic foraminiferal Mg/Ca ratios between 6 and 12 mmol/mol [*Rosenthal et al.*, 2000; *Lear et al.*, 2003; *Reuning et al.*, 2005]. As these samples originated from carbonate platform sediments from shallow core locations, they were interpreted as being influenced by carbonate diagenesis.

[35] Similarly, as foraminiferal Sr/Ca and Mg/Ca ratios are positively correlated after 4.5 Ma ($r^2$ = 0.58), foraminiferal Sr/Ca ratios appear to increase when sedimentary aragonite is low. The range of Sr/Ca ratios of 1.35–1.58 mmol/mol after 4.5 Ma is higher (~12%) than the range of Sr/Ca ratios for the interval before 4.5 Ma (1.25–1.40 mmol/mol), suggesting that dissolution of Sr-rich aragonite and subsequent carbonate reprecipitation from Sr-enriched pore waters onto the foraminiferal

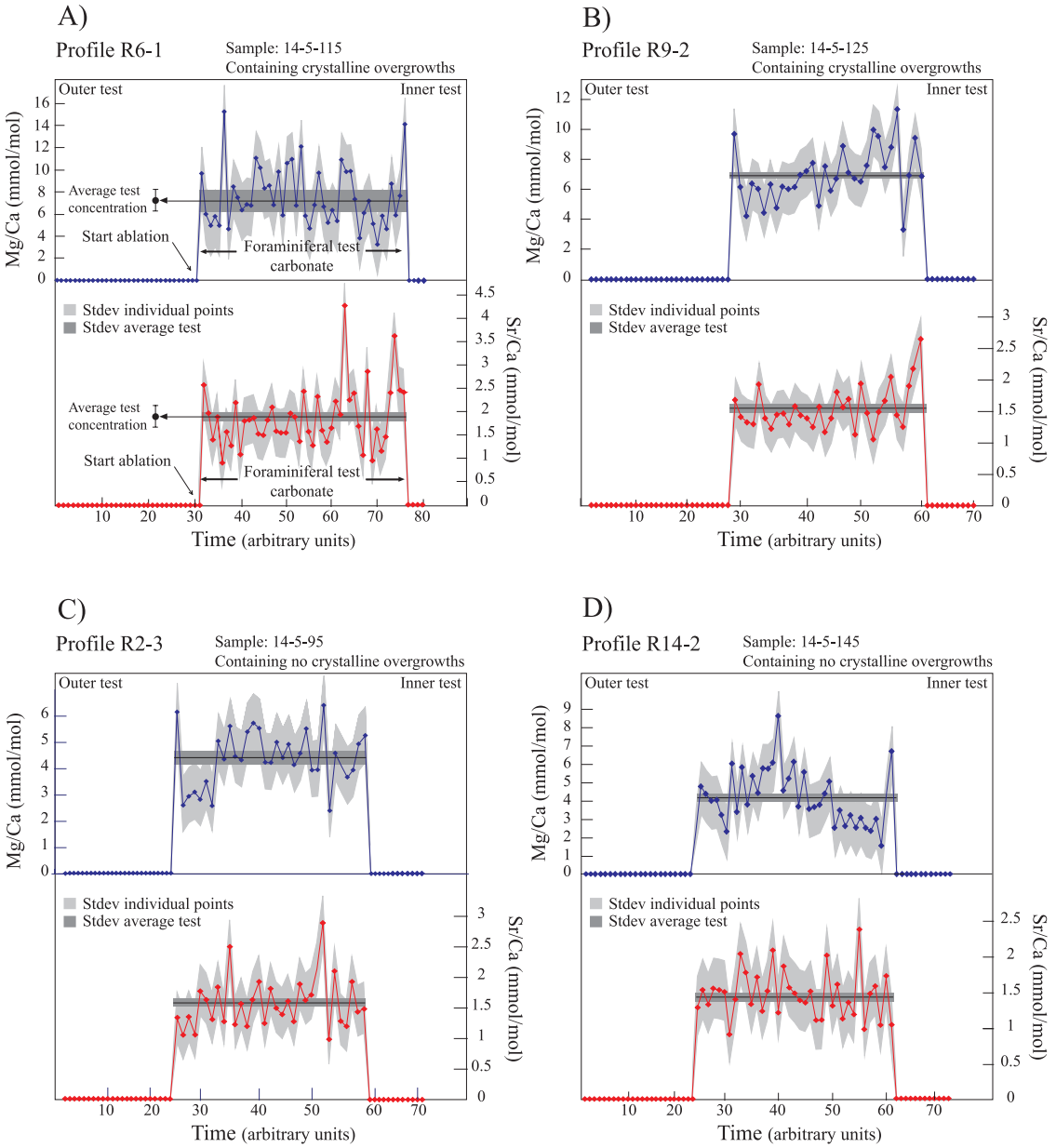


**Figure 7.** Results from LA-ICP-MS for samples with crystalline overgrowths and for samples without crystalline overgrowths. Measurements were performed on cleaned tests of the planktonic foraminifer *G. sacculifer*. All profiles are ablated from the outer side of the test toward the inner side. Time in arbitrary units represents the duration of the ablation process. Dark gray bar shows the standard deviation of the average Mg/Ca and Sr/Ca ratio for the entire profile. Light gray shaded area shows the standard deviation for the single data points. (a and b) Ablation profiles for Mg/Ca and Sr/Ca through samples with crystalline overgrowths (samples 14-5-115 and 14-5-125). (c and d) Ablation profiles for Mg/Ca and Sr/Ca through samples without crystalline overgrowths (samples 14-5-95 and 14-5-145). (e) *G. sacculifer* test, showing an ablation crater formed by LA-ICP-MS analysis (photo taken at Utrecht University, Netherlands).

surfaces took place. This increase in foraminiferal Sr/Ca is too large to be attributed to a change in $Sr/Ca_{seawater}$. A reconstruction by *Lear et al.* [2003] showed an increase in $Sr/Ca_{seawater}$ of less than 5% between the late Miocene and the present. Hence we used LA-ICP-MS to quantify the element concentrations within these diagenetic overgrowths to assess whether these diagenetic overgrowths caused the high element/Ca ratios.

(E)

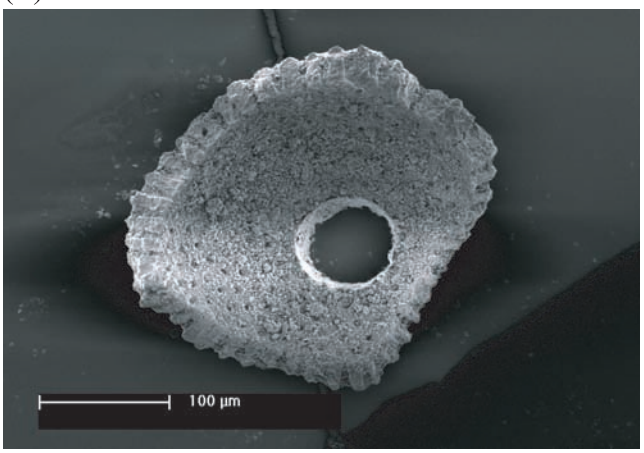


**Figure 7.** (continued)

[36] High-resolution elemental profiles across the chamber walls of *G. sacculifer* performed by LA-ICP-MS [*Eggins et al.*, 2003; *Reichart et al.*, 2003; *Hathorne et al.*, 2003] revealed that Mg/Ca distribution patterns are similar both for specimens from samples with and without crystalline overgrowths (Figure 7). Since the data acquisition of the laser ablation measurements is continuous the first 2–3 data points during ablation can safely be assumed to represent primarily the crystalline overgrowths. The similar Mg/Ca ratios of these points in comparison with the remainder of the foraminiferal test indicate that the crystalline overgrowth is not significantly enriched in Mg and therefore appears not to be responsible for the high bulk Mg/Ca ratios. This, however, does not exclude the possibility of other diagenetic alterations of the bulk Mg/Ca ratios such as partial recrystallization or diffusion of Mg into the tests [*Hover et al.*, 2001].

[37] The similar lack of a significant trace metal enrichment in the observed coatings is also indicated by the profiles for Sr/Ca (Figure 7). Although we would have expected that the crystalline overgrowths are represented by elevated Sr/Ca levels due to the origin from aragonite and the clear correlation between Sr/Ca and aragonite, only slight intratest (up to ~1 mmol/mol) elevations in Sr/Ca were detected (Figures 7a and 7b). This can possibly be explained such that the absolute increase in foraminiferal Sr/Ca after 4.5 Ma in comparison with the older samples was significant but only ~12%. We argue that the expected increase in Sr/Ca in the crystalline overgrowths has not been captured by the laser ablation measurements as the relative standard deviation of the laser

**Table 2a.** Measured Properties of Site 1000[a]

| Specifications Site 1000 | Value | Reference |
|---|---|---|
| Sr pore water | 1771 $\mu$M | *Lyons et al.* [2000] |
| Ca pore water | 10.5 mM | *Lyons et al.* [2000] |
| Mg pore water | 33.9 mM | *Lyons et al.* [2000] |
| Sr/Ca pore water | 168.7 mmol/mol | *Lyons et al.* [2000] |
| Mg/Ca pore water | 3230 mmol/mol | *Lyons et al.* [2000] |
| Averaged maximum $Sr/Ca_{foram}$ < 4.05 Ma | 1.55 mmol/mol | this study |
| Averaged maximum $Sr/Ca_{foram}$ > 4.5 Ma | 1.36 mmol/mol | this study |
| Averaged maximum $Mg/Ca_{foram}$ < 4.05 Ma | 6.33 mmol/mol | this study |

[a] Pore water data (Sample 15-3-145, 4.202 Ma) are from *Lyons et al.* [2000] and are used to calculate the composition of the inorganic calcite. "Average maximum of the contaminated $Sr/Ca_{foram}$" refers to the average Sr/Ca ratio of those samples which show crystalline overgrowths. "Average maximum of the uncontaminated $Sr/Ca_{foram}$" refers to the average Sr/Ca ratio of the samples from the older, uncontaminated part of the record, but only those from the maximum values. "Average maximum of the contaminated $Mg/Ca_{foram}$" refers to the average Mg/Ca ratio of those samples which show crystalline overgrowths.

**Table 2b.** Possible Distribution Coefficients for Mg[a]

| Distribution Coefficient Mg (Inorganic Calcite) | Reference | $Mg/Ca_{crystal}$,[b] mmol/mol |
|---|---|---|
| 0.0008 | *Baker et al.* [1982] | 2.58 |
| 0.004 | *Delaney* [1989] | 12.92 |
| 0.012 | *Mucci and Morse* [1983] | 38.76 |

[a] By using different distribution coefficients for Mg and the pore water composition, the possible Mg/Ca ratios of the inorganic calcite are calculated.
[b] $Mg/Ca_{crystal} = D * Mg/Ca_{solution}$.

ablation measurements has the same order of magnitude (~10%) as the diagenetically induced enrichment.

[38] Pore water chemistry can provide indications on the composition of the diagenetically precipitated inorganic calcite (Tables 2a–2d). Calculation of the Mg/Ca ratio in the crystalline overgrowths is dependant on the distribution coefficient used for Mg [*Tripati et al.*, 2003; *Reuning et al.*, 2005]. However, there is a large variety of Mg distribution coefficients either assessed from sediments or experimentally derived ranging between $0.8 * 10^{-3}$ and $12.3 * 10^{-3}$ [*Baker et al.*, 1982; *Mucci and Morse*, 1983; *Delaney*, 1989; *Morse and Bender*, 1990; *Andreasen and Delaney*, 2000] (Table 2b). *Morse and Bender* [1990] and *Delaney* [1989] demonstrated that such variability can be explained by changing element concentrations in pore water during the recrystallization process.

[39] There are several arguments to use Sr/Ca, instead of Mg/Ca, to calculate the possible composition of the crystalline overgrowths. Firstly, the pore water composition for the studied interval of Site 1000 is mainly determined by selective dissolution of aragonite which is relatively enriched in Sr (1000–10,000 ppm). Secondly, the distribution coefficient of Sr is much better constrained (0.015–0.06) than the distribution coefficient of Mg [*Baker et al.*, 1982; *Delaney*, 1989; *Morse and Bender*, 1990] (Table 2c). Several experiments have shown that for the recrystallization of calcite, which is typically a very slow process, the effect of changing precipitation rate yields distribution coefficients for Sr between 0.03 and 0.06 [*Katz et al.*, 1972; *Baker et al.*, 1982; *Pingitore and Eastman*, 1986]. Thirdly, the range of Sr/Ca ratios in modern planktonic foraminifers is small (1.25–1.40 mmol/mol). Such a range is typically found in samples >4.5 Ma having no crystalline overgrowths (average = 1.36 mmol/mol). We therefore assume that the 12% increase in Sr/Ca in the samples <4.5 Ma, which show crystalline overgrowths (average = 1.55 mmol/mol), is due to aragonite dissolution and subsequent reprecipitation. The assumption that this increase is solely due to diagenesis can be used to estimate the proportion of diagenetic calcite with respect to the initial foraminiferal calcite [*Lohmann*, 1995; *Reuning et al.*, 2005] (Table 2c). Since the process of recrystallization occurs over long time periods and accordingly over a large range of sediment depths, the conditions under which the recrystallization occurs, like changing temperature or changing pore water concentrations, can change significantly. Distribution coefficients which are determined after pore water chemistry therefore only represent the "last stage" in the process and will yield different coefficients than those which are determined after the composition of inorganic precipitates, either sediment-derived or experimentally derived.

[40] We used the estimation of the amount of inorganically precipitated calcite, based on Sr/Ca, to calculate the possible composition of the primary Mg/Ca ratio of the foraminifer [*Lohmann*, 1995] (Table 2d). The average Mg/Ca ratio of the affected samples (6.33 mmol/mol) was used as bulk value. Although we cannot completely rule out the possibility of diagenetically induced changes within the test, the SEM analyses only show diagenetic crystals on the inner side of the tests. This makes the estimations using 16.1% diagenetic calcite seem too high (Table 2d). The distribution coefficient for naturally precipitated inorganic calcite tends to be lower than the one for experimentally precipitated calcite [*Baker et al.*, 1982; *Delaney*, 1989] (Table 2b), suggesting that the estimations based on the experimentally derived distribution coefficient of *Mucci and Morse* [1983] are possibly not

**Table 2c.** Possible Distribution Coefficients for Sr[a]

| Distribution Coefficient Sr (Inorganic Calcite) | Reference | $Sr/Ca_{crystal}$,[b] mmol/mol | Mass Percentage Crystal,[c] % |
|---|---|---|---|
| 0.015 | *Delaney* [1989] | 2.53 | 16.1 |
| 0.040 | *Baker et al.* [1982] | 6.75 | 3.4 |
| 0.050 | *Delaney* [1989] | 8.43 | 2.7 |
| 0.060 | *Katz et al.* [1972] | 10.12 | 2.1 |

[a] By using different distribution coefficients for Sr and the pore water composition, the possible Sr/Ca ratios of the inorganic calcite are calculated. Using these compositions in combination with the measured $Sr/Ca_{foram}$, the mass percentage of the diagenetic overprint of the bulk analyzed foraminifer is calculated [*Lohmann*, 1995].
[b] $Sr/Ca_{crystal} = D * Sr/Ca_{solution}$.
[c] $M_{crystal} = (Sr/Ca_{bulk} - Sr/Ca_{prim})/(Sr/Ca_{second} - Sr/Ca_{prim})$.

**Table 2d.** Calculated Compositions of the Inorganic Calcite[a]

| | Mass Percentage of the Crystals, %[b] | | | |
|---|---|---|---|---|
| | 16.1 | 3.4 | 2.7 | 2.1 |
| Mg/Ca of the crystals, mmol/mol | | | | |
| 2.58 | 7.05 | **6.46** | **6.43** | **6.41** |
| 12.92 | 5.06 | **6.10** | **6.15** | **6.19** |
| 38.76 | 0.11 | 5.18 | 5.43 | 5.63 |

[a] Original Mg/Ca ratios of the contaminated foraminiferal tests. Combining the mass percentage of the crystalline overgrowth with the calculated Mg/Ca ratios of the overgrowth, the Mg/Ca ratios of the original contaminated foraminiferal tests are calculated [*Lohmann*, 1995]. These calculations provide an indication that the crystalline overgrowth does not necessarily elevate the bulk Mg/Ca ratios.

[b] $Mg/Ca_{prim} = (Mg/Ca_{bulk} - (Mass_{crystal} * Mg/Ca_{crystal}))/(1 - Mass_{crystal})$.

realistic either. These two limitations leave a range of possible Mg/Ca ratios for the primary calcite (highlighted in Table 2d with bold text) which differs only slightly from the analyzed bulk values. Thus the exercise on estimating the composition of the primary Mg/Ca ratio in the foraminiferal tests is not conclusive. The theoretical composition of the inorganic precipitates is potentially able to alter the Mg/Ca ratio both to lower and higher values. As the contribution of the diagenetic influence is not conclusive in causing the anomalously Mg/Ca ratios, and the $\delta^{18}O$ record is dominated by changes in salinity (section 4.1) [*Steph et al.*, 2006] we explored the influence of large salinity variations on the Mg/Ca in the next section.

## 5. Correction of Mg/Ca for the Potential Influence of Salinity

[41] Both the positive relationship between the Mg/Ca and $\delta^{18}O_{G.\ sacculifer}$ records (Figure 3), and the suggested increase in Caribbean SSS after 4.5 Ma [*Haug et al.*, 2001; *Steph et al.*, 2006] basically suggest that the planktonic $\delta^{18}O$ record is dominated by variations in SSS. Cultivating experiments with *G. sacculifer* revealed a positive relationship between foraminiferal Mg/Ca and salinity [*Nürnberg et al.*, 1996], suggesting a 7% to 10% increase in Mg/Ca per salinity unit. *Lea et al.* [1999] concluded from cultivating experiments with *Orbulina universa* that a change of 1 salinity unit causes a 4 ± 3% increase in Mg/Ca.

[42] The influence of changes in ice volume on the $\delta^{18}O$ record is negligible for the studied time interval. Glacial to interglacial variations in global ice volume during the early Pliocene were only on the order of 0.15–0.25‰ [*Hodell and Warnke*, 1991; *Kennett and Hodell*, 1993; *Tiedemann et al.*, 1994; *Shackleton et al.*, 1995; *Mix et al.*, 1995] and occurred on obliquity-related cyclicities instead of the precession-related cyclicities encountered in the critical time interval. The temperature effect cannot be extracted from the $\delta^{18}O$ record because the Mg/Ca temperatures are subject of the correction and no other independent temperature estimate is available. Nevertheless, as the influence of temperature and salinity are working in opposite directions on the $\delta^{18}O$, the $\delta^{18}O$ and Mg/Ca records show a positive correlation to each other, and as the $\delta^{18}O$ record is dominated by variations in SSS [*Steph et al.*, 2006], the variations in $\delta^{18}O$ can be assumed to be minimum changes in salinity.

[43] We converted the $\delta^{18}O$ fluctuations of up to 1.4‰ for the time interval 4.5–3.9 Ma in salinity variations on the order of maximum three salinity units, when applying *Broecker*'s [1989] rule of thumb: 1‰ $\delta^{18}O$ = 2 salinity units (Figure 8). Subsequently, we corrected the Mg/Ca record for the effect of these minimum salinity changes by using a 7% increase in Mg/Ca with 1 unit increase in salinity [*Nürnberg et al.*, 1996]. Salinity variations of up to 3 salinity units deduced from the planktonic $\delta^{18}O$ record would therefore result in an overestimation in Mg/Ca of maximum ~21%, equal to ~1.5 mmol/mol. Correcting Mg/Ca for this overestimation leads to $SST_{Mg/Ca}$ estimates which are up to 3.5°C lower. After the correction $SST_{Mg/Ca}$ shows maximum amplitudes of ~4.5°C, and maximum $SST_{Mg/Ca}$ estimates up to 32°C (in comparison to 35°C and 5°C amplitude before the correction). The average $SST_{Mg/Ca}$ increase from 4.5–3.9 Ma is ~3°C (Figure 8). As this correction is only a first estimation, the absolute values are probably still too high. With the availability of an independent temperature proxy the absolute changes in salinity could be determined and used to correct the Mg/Ca record. A first effort was made by *Gussone et al.* [2004], who used low-resolution early Pliocene records to isolate the salinity component in $\delta^{18}O$ by subtracting temperature estimates based on $\delta^{44}Ca$ on *G. sacculifer*, and subsequently correcting Mg/Ca for the influence of salinity.

[44] In summary, we state that the estimation of a 3°C increase in $SST_{Mg/Ca}$ between 4.5 and 3.9 Ma

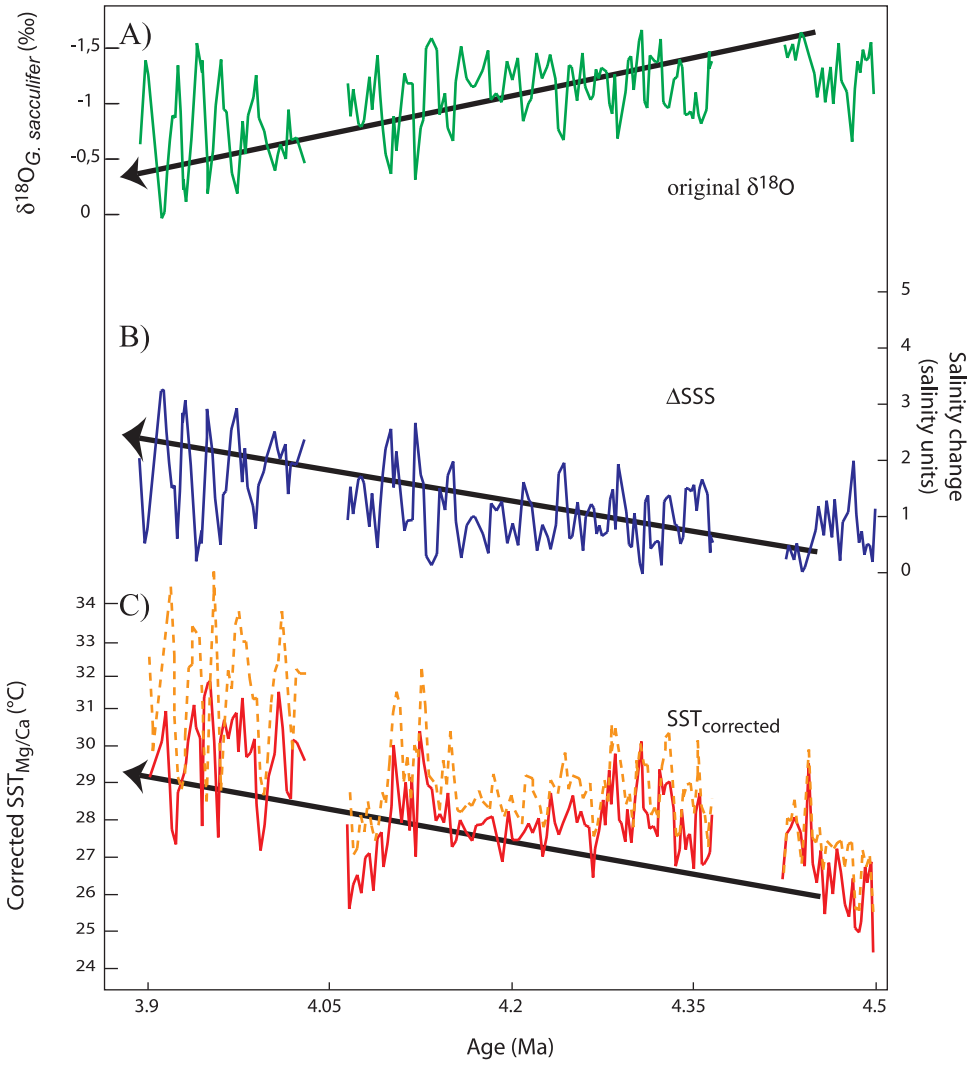


**Figure 8.** Correction of the Mg/Ca record of *G. sacculifer* of Site 1000 for the time interval 4.5–3.9 Ma for the influence of salinity. Arrows indicate trends associated with the restriction of upper ocean water masses between the Pacific and the Caribbean since 4.5 Ma. (a) Original $\delta^{18}$O record of *G. sacculifer* for Site 1000 [*Steph et al.*, 2006]. (b) Change in salinity, calculated using the basic rule that $\Delta$1‰ $\delta^{18}$O = $\Delta$2 salinity units salinity [*Broecker*, 1989]. We assumed that the variations in the $\delta^{18}$O record only represent changes in salinity (see text for explanation). (c) Corrected $SST_{Mg/Ca}$ record. Mg/Ca ratios were corrected by using a 7% increase in Mg/Ca per 1 unit increase in salinity [*Nürnberg et al.*, 1996]. Dotted line shows the original, uncorrected Mg/Ca record.

as a result of the salinity correction can be tested for its paleoceanographical validity by only considering the minimum Mg/Ca values for this interval. The minimum Mg/Ca values correlate with the minimum $\delta^{18}O_{G.\ sacculifer}$ values and therefore reflect ages where SSS did not differ significantly from the period before 4.5 Ma. Therefore these samples are considered not to be affected by the influence of salinity on Mg/Ca. Also, since the minimum Mg/Ca values do neither contain any indication for crystalline overgrowths nor are correlated with those intervals where diagenesis occurred, they can be considered as reflecting a primary temperature signal. Accordingly, the trend in $SST_{Mg/Ca}$ between 4.5 and 3.9 Ma, indeed, shows a warming with ~2.5°C (Figures 3 and 8), possibly showing the initiation of the Western Atlantic Warm Pool.

## 6. Conclusions

[45] We constructed a high-resolution Mg/Ca record on the planktonic foraminifer *G. sacculifer* in order to explore the change in sea surface

temperature (SST) due to the shoaling of the Isthmus of Panama as well as the impact of secondary factors like diagenesis and large salinity fluctuations. The study covers the latest Miocene and the early Pliocene (5.6–3.9 Ma) and was combined with $\delta^{18}O$ to isolate changes in sea surface salinity (SSS). Our results imply a relatively uniform $SST_{Mg/Ca}$ pattern of 26.5°C–29°C for the time interval 5.6–4.5 Ma, and moderate fluctuations in $\delta^{18}O$ representing small fluctuations in global ice volume, salinity, and SST.

[46] After 4.5 Ma, we show a positive correlation between Mg/Ca and $\delta^{18}O$, high $SST_{Mg/Ca}$ are paralleled by high $\delta^{18}O$ values on a precessional timescale. Mg/Ca ratios reach up to ~7 mmol/mol, which would translate into temperatures of ~35°C with amplitudes of up to 5°C. Amplitudes in $\delta^{18}O$ reach 1.4‰ with a general increasing trend toward higher values. We discussed two possible explanations for the anomalous Mg/Ca ratios, a diagenetic overprint on the foraminiferal tests and the possible influence of large salinity variations on Mg/Ca.

[47] SEM analyses of foraminiferal tests of *G. sacculifer* showing anomalously high Mg/Ca ratios reveal crystalline overgrowths. Foraminiferal Sr/Ca ratios, carbonate mineralogy, and calcareous nannofossil analysis suggest that diagenetically induced aragonite dissolution and reprecipitation caused these overgrowths. LA-ICP-MS measurements, however, show that the crystalline overgrowths do not contain significantly higher Mg/Ca ratios than the foraminiferal tests. Also, calculations based on pore water data from Site 1000 result in possible Mg/Ca ratios of the crystalline overgrowths which can both be higher and lower than the primary Mg/Ca ratios. Hence it appears that even though a diagenetic overprint is present, it possibly is not responsible for the anomalous Mg/Ca ratios. However, we do acknowledge that our approach does not exclude alternative diagenetic processes like diffusion or (partial) recrystallization, which might have caused alteration throughout the foraminiferal tests.

[48] The large fluctuations on precessional timescales in the $\delta^{18}O$ record of Site 1000 correlate well with the diagenetically induced cyclicities in aragonite, Sr/Ca, and productivity. As these precession cycles are not present in the $\delta^{18}O$ of *G. sacculifer* in the southern Caribbean Site 999, it is possible that the $\delta^{18}O$ signal of Site 1000 contains a diagenetic overprint. The same comparison, however, of the planktonic foraminifer *G. crassaformis* and the benthic foraminifer *C. wuellerstorfi* $\delta^{18}O$ records between Site 999 and 1000 shows an absence of precession cycles and comparable values, arguing against a diagenetic overprint on $\delta^{18}O$. Also, the large fluctuations in SSS were previously interpreted paleoceanographically by the precessional alternation between relatively fresh Pacific surface water masses and higher saline Atlantic surface water masses bathing Site 1000 [*Steph et al.*, 2006].

[49] The large fluctuations in SSS as suggested by the $\delta^{18}O$ record provide an alternative explanation to the anomalous Mg/Ca ratios after 4.5 Ma [*Steph et al.*, 2006]. Cultivating experiments suggest that salinity exerts an influence on foraminiferal Mg/Ca [*Nürnberg et al.*, 1996; *Lea et al.*, 1999]. In case the $\delta^{18}O$ record is assumed to represent minimal changes in salinity, the Mg/Ca record can be corrected for the influence of salinity. The resulting corrected Mg/Ca record shows an increase in Caribbean $SST_{Mg/Ca}$ after 4.5 Ma of ~3°C.

[50] In summary, we state that the Mg/Ca record of Site 1000 after 4.5 Ma can only reliably be considered for paleoceanographical purposes when the minimum values of the record are converted into SST. These are the samples which do not contain any signs of diagenetic overprint, and represent the $\delta^{18}O$ values which do not indicate large variations in SSS in comparison with part of the record before 4.5 Ma.

## Acknowledgments

[51] This research used samples and data provided by the Ocean Drilling Program, which is sponsored by the U.S. National Science Foundation and participating countries under management of Joint Oceanographic Institutions. This study was performed within DFG-Research Unit "Impact of Gateways on Ocean Circulation, Climate, and Evolution" (FOR451/1-1 TP B2). We would like to thank Silvia Koch, Kerrin Wittmaack, Nicole Gau, Jutta Heintze, Kristin Nass, Beate Bader, Ute Schuldt, and Gijs Nobbe for sample preparation and laboratory assistance. We gratefully thank Marcus Regenberg, Joachim Schönfeld, Martin Ziegler, Stephan Steinke, and two anonymous reviewers for their useful comments and the improvement of the manuscript.

## References

Andreasen, G. H., and M. L. Delaney (2000), Lithologic controls on calcite recrystallizations in Cenozoic deep-sea sediments, *Mar. Geol.*, *163*, 109–124.

Archer, D. E. (1996), An atlas of the distribution of calcium carbonate in sediments of the deep sea, *Global Biogeochem. Cycles.*, *10*, 159–174.

Baker, P., J. M. Gieskes, and H. Elderfield (1982), Diagenesis of carbonates in deep-sea sediments evidence from Sr/Ca

ratios and interstitial dissolved $Sr^{2+}$ data, *J. Sediment. Petrol.*, *52*, 71–82.

Barker, S., M. Greaves, and H. Elderfield (2003), A study of cleaning procedures used for foraminiferal Mg/Ca paleothermometry, *Geochem. Geophys. Geosyst.*, *4*(9), 8407, doi:10.1029/2003GC000559.

Bartoli, G., M. Sarnthein, and M. Weinelt (2005), Final closure of Panama and the onset of Northern Hemisphere glaciation, *Earth Planet. Sci. Lett.*, *237*, 33–44.

Beaufort, L., Y. Lancelot, P. Camberlin, O. Cayre, E. Vincent, F. Bassinot, and L. Labeyrie (1997), Insolation cycles as a major control of equatorial Indian Ocean primary production, *Science*, *278*, 1451–1454.

Berner, R. A., A. C. Lasaga, and R. M. Garrels (1983), The carbonate-silicate geochemical cycle and its effect on atmospheric carbon dioxide over the past 100 million years, *Am. J. Sci.*, *283*, 641–683.

Bickert, T., W. B. Curry, and G. Wefer (1997), Late Pliocene to Holocene (2.6–0 Ma) western equatorial Atlantic deep-water circulation: Inferences from benthic stable isotopes, Leg 154, *Proc. Ocean Drill. Program Sci. Results*, *154*, 239–254.

Billups, K., and D. P. Schrag (2003), Application of benthic foraminiferal Mg/Ca ratios to questions of Cenozoic climate change, *Earth Planet. Sci. Lett.*, *209*, 181–195.

Billups, K., A. C. Ravelo, and J. C. Zachos (1998), Early Pliocene climate: A perspective from the western equatorial Atlantic warm pool, *Paleoceanography*, *13*, 459–470.

Billups, K., A. C. Ravelo, J. C. Zachos, and R. D. Norris (1999), Link between oceanic heat transport, thermohaline circulation, and the Intertropical Convergence Zone in the early Pliocene Atlantic, *Geology*, *27*, 319–322.

Boyle, E. A. (1983), Manganese carbonate overgrowths on foraminiferal tests, *Geochim. Cosmochim. Acta*, *47*, 1815–1819.

Boyle, E. A., and L. D. Keigwin (1985), Comparison of Atlantic and Pacific paleochemical records for the lat 215,000 years: Changes in deep ocean circulation and chemical inventories, *Earth Planet. Sci. Lett.*, *76*, 135–150.

Broecker, W. S. (1989), The salinity contrast between the Atlantic and Pacific oceans during glacial time, *Paleoceanography*, *4*, 207–212.

Broecker, W. S., and T. H. Peng (Eds.) (1982), *Tracers in the Sea*, 690 pp., Eldigio, Palisades, N. Y.

Brown, S. J. (1996), Controls on the trace metal chemistry of foraminiferal calcite and aragonite, 231 pp., Ph.D. thesis, Univ. of Cambridge, Cambridge, UK.

Brown, S. J., and H. Elderfield (1996), Variations in Mg/Ca and Sr/Ca ratios of planktonic foraminifera caused by post-depositional dissolution: Evidence of shallow Mg-dependent dissolution, *Paleoceanography*, *11*(5), 543–551.

Cronin, T. M., R. Whatley, A. Wood, A. Tsukagoshi, N. Ikeya, E. M. Brouwers, and W. M. Briggs, Jr. (1993), Microfaunal evidence for elevated Pliocene temperatures in the Arctic Ocean, *Paleoceanography*, *8*, 161–173.

Crowley, T. J. (1996), Pliocene climates: The nature of the problem, *Mar. Micropaleontol.*, *27*, 3–12.

Crudeli, D. (2005), Early Pliocene evolution of coccolithophores in the Caribbean Sea: Taxonomy, biostratigraphy, paleoecology and paleoceanography, Ph.D. thesis, Univ. of Kiel, Kiel, Germany.

Crudeli, D., and H. Kinkel (2004), *Reticulofenestra calicis* n. sp., an unusual small reticulofenestrid coccolith from the Lower Pliocene of the South Caribbean Sea, *Micropaleontology*, *50*(4), 369–379.

de Garidel-Thoron, T., L. Beaufort, B. K. Linsley, and S. Dannenmann (2001), Millennial-scale dynamics of the East Asian winter monsoon during the last 200,000 years, *Paleoceanography*, *16*, 1–12.

Dekens, P. S., D. W. Lea, D. K. Pak, and H. J. Spero (2002), Core top calibration of Mg/Ca in tropical foraminifera: Refining paleotemperature estimation, *Geochem. Geophys. Geosyst.*, *3*(4), 1022, doi:10.1029/2001GC000200.

Delaney, M. L. (1989), Temporal changes in interstitial water chemistry and calcite recrystallization in marine sediments, *Earth Planet. Sci. Lett.*, *95*, 23–37.

Dix, G. R., and H. T. Mullins (1992), Shallow-burial diagenesis of deep-water carbonates, northern Bahamas: Results from deep-ocean drilling transects, *Geol. Soc. Am. Bull.*, *104*, 303–315.

Dowsett, H. J., J. Barron, and R. Poore (1996), Middle Pliocene sea surface temperatures: A global reconstruction, *Mar. Micropaleontol.*, *27*, 13–25.

Driscoll, N. W., and G. H. Haug (1998), A short circuit in thermohaline circulation: A cause for Northern Hemisphere glaciation?, *Science*, *282*, 436–438.

Eggins, S., P. De Deckker, and J. Marshall (2003), Mg/Ca variation in planktonic foraminifera shells: Implications for reconstruction of paleo sea water temperature and habitat migration, *Earth Planet. Sci. Lett.*, *212*(3–4), 291–306.

Elderfield, H., and G. Ganssen (2000), Past temperature and $\delta^{18}O$ of surface ocean waters inferred from foraminiferal Mg/Ca ratios, *Nature*, *405*, 442–445.

Elderfield, H., and A. Schultz (1996), Mid-ocean ridge hydrothermal fluxes and the chemical composition of the ocean, *Annu. Rev. Earth Planet. Sci.*, *24*, 191–224.

Fairbanks, R. G., M. Sverdlove, R. Free, P. H. Wiebe, and A. W. H. Be (1982), Vertical distribution and isotopic fractionation of living planktonic foraminifera from the Panama Basin, *Nature*, *298*, 841–844.

Frank, T. D., and K. Bernet (2000), Isotopic signature of burial diagenesis and primary lithological contrasts in periplatform carbonates (Miocene, Great Bahama Bank), *Sedimentology*, *47*, 1119–1134.

Gieskes, J. M., and J. R. Lawrence (1981), Alteration of volcanic matter in deep sea sediments: Evidence from the chemical composition of interstitial waters from deep sea drilling cores, *Geochim. Cosmochim. Acta*, *45*, 1687–1703.

Greaves, M., S. Barker, C. Daunt, and H. Elderfield (2005), Accuracy, standardization, and interlaboratory calibration standards for foraminiferal Mg/Ca thermometry, *Geochem. Geophys. Geosyst.*, *6*, Q02D13, doi:10.1029/2004GC000790.

Groeneveld, J., S. Steph, R. Tiedemann, D. Garbe-Schönberg, D. Nürnberg, and A. Sturm (2006), Pliocene mixed layer oceanography for Site 1241, using combined Mg/Ca and $\delta^{18}O$ analyses of *Globigerinoides sacculifer*, *Proc. Ocean Drill. Program Sci. Results*, *202*, 27 pp. (Available at http://www-odp.tamu.edu/publications/202_SR/209/209.htm)

Günther, D., R. Frischknecht, C. A. Heinrich, and H. J. Kahlert (1997), Capabilities of a 193 nm ArF excimer laser for LA-ICP-MS micro analysis of geological materials, *J. Anal. At. Spectrom.*, *12*, 939–944.

Gussone, N., A. Eisenhauer, R. Tiedemann, G. H. Haug, A. Heuser, B. Bock, F. Th. Nägler, and A. Müller (2004), Reconstruction of Caribbean sea surface temperature and salinity fluctuations in response to the Pliocene closure of the Central American Gateway and radiative forcing, using $\delta^{44/40}Ca$, $\delta^{18}O$ and Mg/Ca ratios, *Earth Planet. Sci. Lett.*, *227*, 201–214.

Hathorne, E. C., O. Alard, R. H. James, and N. W. Rogers (2003), Determination of intratest variability of trace elements in foraminifera by laser ablation inductively coupled

plasma-mass spectrometry, *Geochem. Geophys. Geosyst.*, *4*(12), 8408, doi:10.1029/2003GC000539.

Haug, G. H., and R. Tiedemann (1998), Effect of the formation of the Isthmus of Panama on Atlantic Ocean thermohaline circulation, *Nature*, *393*, 673–676.

Haug, G. H., R. Tiedemann, R. Zahn, and A. C. Ravelo (2001), Role of Panama uplift on oceanic freshwater balance, *Geology*, *29*, 207–210.

Hodell, D. A., and D. A. Warnke (1991), Climate evolution of the Southern Ocean during the Pliocene epoch from 4.8 to 2.6 million years ago, *Quat. Sci. Rev.*, *10*, 205–214.

Hover, V. C., L. M. Walter, and D. R. Peacor (2001), Early marine diagenesis of biogenic aragonite and Mg-calcite: New constraints from high-resolution STEM and AEM analyses of modern platform carbonates, *Chem. Geol.*, *175*, 221–248.

Kameo, K., and T. Sato (2000), Biogeography of Neogene calcareous nannofossils in the Caribbean and the eastern equatorial Pacific–floral response to the emergence of the Isthmus of Panama, *Mar. Micropaleontol.*, *39*, 201–218.

Katz, A., E. Sass, A. Starinsky, and H. D. Holland (1972), Strontium behavior in the aragonite-calcite transformation: An experimental study at 40–98°C, *Geochim. Cosmochim. Acta*, *36*, 481–496.

Keigwin, L. (1982), Isotopic paleoceanography of the Caribbean and east Pacific Role of Panama uplift in late Neogene time, *Science*, *217*, 350–353.

Kennett, J. P., and D. A. Hodell (1993), Evidence for relative climate stability of Antarctica during the early Pliocene: A marine perspective, *Geogr. Ann.*, *75*, 205–220.

Killingley, J. S. (1983), Effects of diagenetic recrystallization on $^{18}O/^{16}O$ values of deep-sea sediments, *Nature*, *301*, 594–597.

Lea, D. W., T. A. Mashiotta, and H. J. Spero (1999), Controls on magnesium and strontium uptake in planktonic foraminifera determined by live culturing, *Geochim. Cosmochim. Acta*, *63*, 2369–2379.

Lea, D. W., D. K. Pak, and H. J. Spero (2000), Climate impact of Late Quaternary equatorial Pacific sea surface temperature variations, *Science*, *289*, 1719–1724.

Lear, C. H., H. Elderfield, and P. A. Wilson (2000), Cenozoic deep-sea temperatures and global ice volumes from Mg/Ca in benthic foraminiferal calcite, *Science*, *287*, 269–272.

Lear, C. H., H. Elderfield, and P. A. Wilson (2003), A Cenozoic seawater Sr/Ca record from benthic foraminiferal calcite and its application in determining global weathering fluxes, *Earth Planet. Sci. Lett.*, *208*, 69–84.

Levitus, S., and T. Boyer (1994), *World Ocean Atlas 1994*, vol. 4, *Temperature*, *NOAA Atlas NESDIS 4*, U.S. Dept. of Commer., Washington, D. C.

Lohmann, G. P. (1995), A model for variation in the chemistry of planktonic foraminifera due to secondary calcification and selective dissolution, *Paleoceanography*, *10*, 445–457.

Lyons, T. W., R. W. Murray, and D. G. Pearson (2000), A comparative study of diagenetic pathways in sediments of the Caribbean Sea: Highlights from pore-water results, *Proc. Ocean Drill. Program Sci. Results*, *165*, 287–298.

Maier-Reimer, E., U. Mikolajewicz, and T. Crowley (1990), Ocean general circulation model sensitivity experiment with an open Central American isthmus, *Paleoceanography*, *5*, 349–366.

Malone, M. J., P. Baker, S. Burns, and P. Swart (1990), Geochemistry of periplatform carbonate sediments, Ocean Drilling Progran Site 716 (Maldives Archipelago, Indian Ocean), *Proc. Ocean Drill. Program Sci. Results*, *115*, 647–659.

Mashiotta, T. A., D. W. Lea, and H. J. Spero (1999), Glacial-interglacial changes in Subantarctic sea surface temperature and $\delta^{18}O$-water using foraminiferal Mg, *Earth Planet. Sci. Lett.*, *170*, 417–432.

Mason, P. R. D., and A. J. G. Mank (2001), Depth-resolved analysis in multi-layered glass and metal materials using laser ablation inductively coupled plasma mass spectrometry (LA-ICP-MS), *J. Anal. At. Spectrom.*, *16*, 1381–1388.

McKenna, V. S., and W. L. Prell (2004), Calibration of the Mg/Ca of *Globorotalia truncatulinoides* (R) for the reconstruction of marine temperature gradients, *Paleoceanography*, *19*, PA2006, doi:10.1029/2000PA000604.

Melim, L. A., H. Westphal, P. K. Swart, G. P. Eberli, and A. Munnecke (2002), Questioning carbonate diagenetic paradigms: Evidence from the Neogene of the Bahamas, *Mar. Geol.*, *185*, 27–53.

Mix, A. C., N. G. Pisias, W. Rugh, J. Wilson, A. Morey, and T. K. Hagelberg (1995), Benthic foraminifer stable isotope record from Site 849 (0–5 Ma): Local and global climate changes, *Proc. Ocean Drill. Program Sci. Results*, *138*, 371–412.

Molfino, B., and A. McIntyre (1990), Precessional forcing of nutricline dynamics in the equatorial Atlantic, *Science*, *249*, 766–769.

Morse, J. W., and M. L. Bender (1990), Partition coefficients in calcite: Examination of factors influencing the validity of experimental results and their application to natural systems, *Chem. Geol.*, *82*, 265–277.

Mottle, M. J., and G. Wheat (1994), Hydrothermal circulation through mid-ocean ridge flanks: Fluxes of heat and magnesium, *Geochim. Cosmochim. Acta*, *58*, 2225–2237.

Mucci, A., and J. W. Morse (1983), The incorporation of $Mg^{2+}$ and $Sr^{2+}$ into calcite overgrowths: Influences of growth rate and solution composition, *Geochim. Cosmochim. Acta*, *47*, 217–233.

Munnecke, A., H. Westphal, J. J. G. Reijmer, and C. Samtleben (1997), Microspar development during early marine burial diagenesis: A comparison of Pliocene carbonates from the Bahamas with Silurian limestones from Gotland (Sweden), *Sedimentology*, *44*, 977–990.

Newell, R. E. (1979), Climate and the ocean, *Am. Sci.*, *67*, 405–416.

Niebler, H. S., H. W. Hubberten, and R. Gersonde (1999), Oxygen isotope values of planktic foraminifera: A tool for the reconstruction of surface water stratification, in *Use of Proxies in Paleoceanography*, edited by G. Fischer and G. Wefer, pp. 165–189, Springer, New York.

Nürnberg, D. (1995), Magnesium in tests of *Neogloboquadrina pachyderma sinistral* from high northern and southern latitudes, *J. Foraminiferal Res.*, *25*, 350–368.

Nürnberg, D. (2000), Taking the temperature of past ocean surfaces, *Science*, *289*, 1698–1699.

Nürnberg, D., J. Bijma, and C. Hemleben (1996), Assessing the reliability of magnesium in foraminiferal calcite as a proxy for water mass temperatures, *Geochim. Cosmochim. Acta*, *60*, 803–814.

Nürnberg, D., A. Müller, and R. R. Schneider (2000), Paleo-sea surface temperature calculations in the equatorial east Atlantic from Mg/Ca ratios in planktic foraminifera: A comparison to sea surface temperature estimates from $U^k_{37}$, oxygen isotopes, and foraminiferal transfer function, *Paleoceanography*, *15*, 124–134.

Pearce, N. J. G., W. T. Perkins, J. A. Westgate, M. P. Gorton, S. E. Jackson, C. R. Neal, and S. P. Chenery (1997), A compilation of new and published major and trace element data for NIST SRM 610 and NIST SRM 612 glass reference materials, *Geostand. Newsl.*, *21*, 115–144.

Pearson, P. N., P. W. Ditchfield, J. Singano, K. G. Harcourt-Brown, C. J. Nicholas, R. K. Olsson, N. J. Shackleton, and M. A. Hall (2001), Warm tropical sea surface temperatures in the Late Cretaceous and Eocene epochs, *Nature*, *413*, 481–487.

Pena, L. D., E. Calvo, I. Cacho, S. Eggins, and C. Pelejero (2005), Identification and removal of Mn-Mg-rich contaminant phases on foraminiferal tests: Implications for Mg/Ca past temperature reconstructions, *Geochem. Geophys. Geosyst.*, *6*, Q09P02, doi:10.1029/2005GC000930.

Philander, S. G. H. (1990), *El Niño, La Niña, and the Southern Oscillation*, 293 pp., Academic, New York.

Pierrehumbert, R. T. (1995), Thermostats, radiator fins, and the local runaway greenhouse, *J. Atmos. Sci.*, *52*, 1784–1806.

Pingitore, N. E., and M. P. Eastman (1986), The coprecipitation of $Sr^{2+}$ with calcite at 25°C and 1 atm., *Geochem. Cosmochim. Acta*, *50*, 2195–2203.

Ramanathan, V., and W. Collins (1991), Thermodynamic regulation of ocean warming by cirrus clouds deduced from observations of the 1987 El Niño, *Nature*, *351*, 27–32.

Reichart, G. J., F. Jorissen, P. Anschutz, and P. R. D. Mason (2003), Single foraminiferal test chemistry records the marine environment, *Geology*, *31*, 355–358.

Reuning, L., J. J. G. Reijmer, C. Betzler, P. Swart, and T. Bauch (2005), The use of paleoceanographic proxies in carbonate periplatform settings: Opportunities and pitfalls, *Sediment. Geol.*, *175*, 131–152.

Ries, J. B. (2004), Effect of ambient Mg/Ca ratio on Mg fractionation in calcareous marine invertebrates: A record of the oceanic Mg/Ca ratio over the Phanerozoic, *Geology*, *32*, 981–984.

Rosenthal, Y., G. P. Lohmann, K. C. Lohmann, and R. M. Sherrell (2000), Incorporation and preservation of Mg in *Globigerinoides sacculifer*: Implications for reconstructing the temperature and $^{18}O/^{16}O$ of seawater, *Paleoceanography*, *15*, 135–145.

Rosenthal, Y., et al. (2004), Interlaboratory comparison study of Mg/Ca and Sr/Ca measurements in planktonic foraminifera for paleoceanographic research, *Geochem. Geophys. Geosyst.*, *5*, Q04D09, doi:10.1029/2003GC000650.

Sadekov, A. Yu., S. M. Eggins, and P. De Deckker (2005), Characterization of Mg/Ca distributions in planktonic foraminifera species by electron microprobe mapping, *Geochem. Geophys. Geosyst.*, *6*, Q12P06, doi:10.1029/2005GC000973.

Schrag, D. P., D. J. DePaolo, and F. M. Richter (1995), Reconstructing past sea surface temperatures: Correcting for diagenesis of bulk marine carbonate, *Geochim. Cosmochim. Acta*, *59*, 2265–2278.

Shackleton, N. J., and M. A. Hall (1997), The Late Miocene stable isotope record, site 926, *Proc. Ocean Drill. Program Sci. Results*, *154*, 367–373.

Shackleton, N. J., M. A. Hall, and D. Pate (1995), Pliocene stable isotope stratigraphy of Site 846, *Proc. Ocean Drill. Program Sci. Results*, *138*, 337–353.

Sigurdsson, H., et al. (1997), *Proceedings of the Ocean Drilling Program*, *Initial Reports*, vol. 165, Ocean Drilling Program, College Station, Tex.

Stanley, S. M., and L. A. Hardie (1998), Secular oscillations in the carbonate mineralogy of reef-building and sediment-producing organisms driven by tectonically forced shifts in seawater chemistry, *Palaeogeogr. Palaeoclimatol. Palaeoecol.*, *144*, 3–19.

Stehli, F. G., and S. D. Webb (Eds.) (1985), *The Great American Biotic Interchange*, 523 pp., Plenum, New York.

Steph, S., R. Tiedemann, M. Prange, J. Groeneveld, D. Nürnberg, L. Reuning, M. Schulz, and G. H. Haug (2006), Changes in Caribbean surface hydrography during the Pliocene shoaling of the Central American Seaway, *Paleoceanography*, *21*, PA4221, doi:10.1029/2004PA001092.

Swart, P. K., and M. Guzikowski (1988), Interstitial water chemistry and diagenesis of periplatform sediments from the Bahamas, ODP Leg 101, *Proc. Ocean Drill. Program Sci. Results*, *101*, 363–380.

Tiedemann, R., and S. O. Franz (1997), Water circulation, chemistry, and terrigenous sediment supply in the Equatorial Atlantic during the Pliocene, 3.3–2.6 Ma and 5–4.5 Ma, *Proc. Ocean Drill. Program Sci. Results*, *154*, 299–318.

Tiedemann, R., M. Sarnthein, and N. J. Shackleton (1994), Astronomic timescale for the Pliocene Atlantic $\delta^{18}O$ and dust flux records of Ocean Drilling Program Site 659, *Paleoceanography*, *9*, 619–638.

Tripati, A. K., M. L. Delaney, J. C. Zachos, L. D. Anderson, D. C. Kelly, and H. Elderfield (2003), Tropical sea-surface temperature reconstruction for the early Paleogene using Mg/Ca ratios of planktonic foraminifera, *Paleoceanography*, *18*(4), 1101, doi:10.1029/2003PA000937.

Waliser, D., and N. Graham (1993), Convective cloud systems and warm-pool sea surface temperatures: Coupled interactions and self-regulation, *J. Geophys. Res.*, *96*(D7), 15,311–15,324.

Wara, M. W., A. C. Ravelo, and M. L. Delaney (2005), Permanent El Niño-like conditions during the Pliocene warm period, *Science*, *309*, 758–761.

Webb, S. D. (1997), The great American faunal interchange, in *Central America: A natural and cultural history*, edited by A. G. Coates, pp. 97–122, Yale Univ. Press, New Haven, Conn.

Wilkinson, B. H., and T. J. Algeo (1989), Sedimentary carbonate record of calcium-magnesium cycling, *Am. J. Sci.*, *289*, 1158–1194.